Title

FMRI hemodynamic response function (HRF) as a novel marker of brain function: applications for understanding obsessive-compulsive disorder pathology and treatment response

Journal

Brain Imaging and Behavior, 15(3)

ISSN

1931-7557

Authors

Rangaprakash, D
Tadayonnejad, Reza
Deshpande, Gopikrishna
et al.

Publication Date

2021-06-01

DOI

10.1007/s11682-020-00358-8

Peer reviewed

HHS Public Access

Author manuscript

Brain Imaging Behav. Author manuscript; available in PMC 2022 June 01.

Published in final edited form as:

Brain Imaging Behav. 2021 June ; 15(3): 1622–1640. doi:10.1007/s11682-020-00358-8.

FMRI hemodynamic response function (HRF) as a novel marker of brain function: applications for understanding obsessive-compulsive disorder pathology and treatment response

D Rangaprakash[1,2], **Reza Tadayonnejad**[1,3], **Gopikrishna Deshpande**[4,5,6,7,8,9,10,11], **Joseph O'Neill**[1], **Jamie D Feusner**[1,*]

[1]Department of Psychiatry and Biobehavioral Sciences, University of California Los Angeles, Los Angeles, CA 90095, USA

[2]Athinoula A. Martinos Center for Biomedical Imaging, Massachusetts General Hospital, Harvard Medical School and Harvard-MIT Health Sciences and Technology, Cambridge, MA 02129, USA

[3]Division of the Humanities and Social Sciences, California Institute of Technology, Pasadena, CA 91125, USA

[4]Department of Electrical and Computer Engineering, Auburn University, Auburn, AL 36849, USA

[5]Department of Psychology, Auburn University, Auburn, AL 36849, USA

[6]Alabama Advanced Imaging Consortium, Auburn University and University of Alabama Birmingham, AL, USA

[7]Center for Health Ecology and Equity Research, Auburn University, Auburn, AL, USA

[8]Center for Neuroscience, Auburn University, Auburn, AL, USA

[9]School of Psychology, Capital Normal University, Beijing, China

[10]Key Laboratory for Learning and Cognition, Capital Normal University, Beijing, China

[11]Department of Psychiatry, National Institute of Mental Health and Neurosciences, Bangalore, India

Abstract

[*]**Correspondence to:** Jamie D. Feusner, M.D., Department of Psychiatry and Biobehavioral Sciences, 300 UCLA Medical Plaza, Suite 2200, Los Angeles, CA, 90095, USA, Tel.: +1 310 206-4951, jfeusner@mednet.ucla.edu.

Conflicts of interest: All the authors (D.R., R.T., G.D, J.O., J.D.F.) declare no conflicts of interest.

Ethical approval: All procedures involving human participants were in accordance with the ethical standards of the institutional research committee and with the 1964 Helsinki declaration and its later amendments or comparable ethical standards. UCLA institutional review board (IRB) approved the study procedures.

Informed consent: Informed consent was obtained from all individual participants included in the study.

The hemodynamic response function (HRF) represents the transfer function linking neural activity with the functional MRI (fMRI) signal, modeling neurovascular coupling. Since HRF is influenced by non-neural factors, to date it has largely been considered as a confound or has been ignored in many analyses. However, underlying biophysics suggests that the HRF may contain meaningful correlates of neural activity, which might be unavailable through conventional fMRI metrics. Here, we estimated the HRF by performing deconvolution on resting-state fMRI data from a longitudinal sample of 25 healthy controls scanned twice and 44 adults with obsessive-compulsive disorder (OCD) before and after 4-weeks of intensive cognitive-behavioral therapy (CBT). HRF response height, time-to-peak and full-width at half-maximum (FWHM) in OCD were abnormal before treatment and normalized after treatment in regions including the caudate. Pre-treatment HRF predicted treatment outcome (OCD symptom reduction) with 86.4% accuracy, using machine learning. Pre-treatment HRF response height in the caudate head and time-to-peak in the caudate tail were top-predictors of treatment response. Time-to-peak in the caudate tail, a region not typically identified in OCD studies using conventional fMRI activation or connectivity measures, may carry novel importance. Additionally, response height in caudate head predicted post-treatment OCD severity ($R=-0.48$, $P= 0.001$), and was associated with treatment-related OCD severity changes ($R=-0.44$, $P=0.0028$), underscoring its relevance. With HRF being a reliable marker sensitive to brain function, OCD pathology, and intervention-related changes, these results could guide future studies towards novel discoveries not possible through conventional fMRI approaches like standard BOLD activation or connectivity.

Keywords

Functional magnetic resonance imaging; fMRI; hemodynamic response function; HRF; obsessive-compulsive disorder; OCD; cognitive-behavioral therapy; CBT; machine learning

INTRODUCTION

Functional magnetic resonance imaging (fMRI) is used extensively for studying the neural correlates of brain functioning, which indirectly measures neural activity through changes in blood oxygenation. Blood oxygenation is impacted by neural activity, as well as neurovascular coupling, blood flow properties, and blood chemistry [1]. The mathematical transfer function model of the neurovascular coupling between local neural activity and the corresponding blood oxygenation level dependent (BOLD) fMRI signal is called the hemodynamic response function (HRF). Studies involving biophysical modeling as well as experimental data have suggested that both neural and non-neural factors control the shape of the HRF [2]. Consequently, the HRF shape has been shown to vary across brain regions and across individuals [1] [3]. It is difficult to delineate the contributions of neural (elaborated below) and non-neural factors towards the HRF shape (such as variable size and density of vasculature, hematocrit, alcohol/caffeine/lipid ingestion, partial volume imaging of veins, global magnetic susceptibilities, slice timing differences and pulse/respiration differences [1] [3] [4] [5] [6]). Given this difficulty, previous studies have adopted two different strategies. One is deconvolving the HRF from the BOLD time series to estimate latent neural activity and in turn building models of the data in this latent space. This is a preferred choice for connectivity models such as dynamic causal modeling (DCM) [7].

Granger causality [8] [9] [10] [11] [12] [13] [14] [15], multivariate dynamical systems (MDS) [16] [17] [18] and resting-state functional connectivity [19]. The second strategy is assuming a standard canonical HRF (typically two gamma functions) as in most task fMRI activation studies, and modeling the error introduced by HRF variability as time and dispersion derivatives using a general linear model (GLM). This is appropriate and can work well since we are interested in the BOLD response time-locked to an external stimulus in task-based studies. However, in resting-state connectivity studies wherein, in the absence of an external input time reference, time-locked covariations between activity in different brain regions are measured, the issue of HRF variability and its effect on connectivity estimates needs to be revisited afresh. Resting-state functional connectivity studies have thus far mostly ignored HRF variability with the notion that the HRF is similar enough in most people that one can ignore intraindividual variability. However, HRF variability has been demonstrated in the brain [3] [1] and recent reports provide evidence that ignoring it can introduce confounds in connectivity estimates [20] [21] [22] [23] [19]. In fact, a recent study found significant HRF variability across healthy individuals that confounded resting-state functional connectivity estimates by as much as 15% [19]. Recent studies in PTSD [24] and autism [21] have shown that HRF impairments in pathological groups are significant enough to confound resting-state connectivity group differences. Earlier studies have demonstrated that lag-based effective connectivity models are viable only after minimizing the HRF confound [25] [26]. With task fMRI, the impact of HRF variability on task-based functional connectivity (e.g. PPI) is yet to be investigated, although evidence suggests that task-based effective connectivity estimates are more accurate after deconvolution [27] [28] [29] [30].

Despite the convention of considering HRF variability as a confound, there is evidence that the HRF carries information relevant to brain function and pathology. Although the complete picture of the underlying biophysics supporting this notion is considerably complex, here we present a simplistic explanation. Local neural activation causes vasodilation and increases cerebral blood flow (CBF), as formulated in the fMRI balloon model [31]. CBF has been found abnormal in psychiatric and neurovascular disorders such as schizophrenia, obsessive-compulsive disorder (OCD), depression, autism spectrum disorder, and dementia [32] [33] [34] [35] [36] [37]. Cerebrovascular reactivity (CVR), the change in CBF in response to neural activity, is closely associated with vasodilation and vasoconstriction of local blood vessels [38], which in turn modulates the HRF [39] [40]. Recent evidence using Doppler ultrasound and infrared spectroscopy suggests abnormalities in CVR in neurological and psychiatric disorders [41] [42]. On the other hand, neurovascular coupling (NVC), which is the coupling between local neural activity and CBF, has also been associated with brain function and pathology [43], and it modulates the HRF [39] [44]. Therefore, neural activity influences the HRF through NVC, CBF, CVR and vasodilation/vasoconstriction mechanisms.

Through NVC, neurometabolic modulators released by glutamatergic and GABAergic interneurons directly and indirectly modulate CBF [45], and subsequently the HRF [46]. Glutamate acts on *N*-methyl-D-aspartate (NMDA) receptors, causing dilation of the blood vessels associated with activated local neurons [47], ultimately impacting the HRF. Higher glutamate concentration results in taller, quicker and narrower HRFs, while higher GABA has the opposite effects [48]. Serotonin (5-hydroxytryptamine) is a vasoconstrictor, which

provides blood-brain barrier permeability for modulating NVC. It modulates the HRF via the neuronal-astrocytic-vascular tripartite functional unit [49]. To summarize, neurometabolic coupling and the balance between inhibitory and excitatory neurotransmitters modulates the HRF through NVC. Fig.1 provides a simplistic illustration of these relationships.

Thus, there are grounds to postulate that the HRF carries information relevant to brain function and pathology. In this paper, we explore whether the HRF is sensitive to brain pathology as well as interventional treatment, as tested in a longitudinal sample of adults with OCD and matched healthy controls (HC). HRF was estimated from resting-state fMRI data.

HRF shape can be characterized by three main parameters [1] [3] (Fig.2): (i) response height (RH), (ii) time-to-peak (TTP), and (iii) full-width at half-max (FWHM). RH is a measure of HRF amplitude. TTP measures the latency and FWHM relates to the duration of the BOLD response. In this study, we assessed two aspects of the HRF to evaluate its utility in neuroimaging: HRF's relevance to pathology and relevance to interventional treatment. Additionally, as preliminary analyses, we assessed HRF's relevance to normal brain function as well as HRF's longitudinal reliability (presented in Supplemental Information S2 and S3 respectively). We acquired resting-state fMRI data at 3T (Fig.3) before and after 4 weeks of no intervention in a sample of 25 HCs and from 44 OCD participants in two sessions: (i) at pre-CBT baseline, and (ii) after 4 weeks of intensive cognitive behavioral therapy (CBT). Voxel-level HRF parameters were obtained by performing deconvolution on pre-processed fMRI data.

We assessed the relevance of the HRF to OCD pathology using the pre-CBT OCD sample, and the relevance of HRF to treatment using the longitudinal OCD sample before and after intensive CBT. Our recent study [50] indicates that resting-state fMRI functional network connectivity tracks CBT-induced brain changes in OCD, but was relatively insensitive to differences between OCD patients and HCs at pre-treatment baseline. Here we sought to evaluate the ability of the HRF to detect such effects. Regional abnormalities in brain metabolism and activation have been observed in OCD that respond to CBT [50] [51] [52] [53] [54] [55] [56] [57] [58] [59].

The current study aimed to determine if HRF aberrations are present in OCD, and to explore links between HRF and clinical symptoms. Specifically, CBF has been found abnormal in OCD [32], as well as altered following CBT treatment in OCD patients [60]. Moreover, CBF modulates the HRF [46]. Hence, there is indirect evidence to hypothesize that HRF is sensitive to brain pathology in OCD and interventional CBT treatment. Many, although not all, of the aforementioned studies in OCD found baseline functional abnormalities in regions in cortico-striato-thalamo-cortical (CSTC) circuits. However, due to the novelty of the current investigative markers of neural function, we did not put forward specific regional hypotheses.

Given this background, we tested two hypotheses: (i) *Hypothesis-1: HRF is sensitive to pathology. OCD individuals would exhibit HRF aberrations compared to HC at baseline*, (ii)

Hypothesis-2: HRF is sensitive to treatment, and predictive of treatment response. Testing this involved the following sub-hypotheses- 2a: *In OCD, CBT would change HRF post-treatment compared to pre-treatment*. 2b: *A subset of the pre-CBT HRF aberrations in OCD would return to normalcy post-CBT*. 2c: *Change in HRF with treatment would be associated with corresponding changes in OCD symptom severity*. 2d: *Pre-treatment HRF parameters would predict treatment outcome in OCD* (reduction in OCD symptom severity) (tested using supervised machine learning classification, simultaneously identifying those regions whose HRF had the highest predictive ability).

When individuals undergo an intervention that improves symptoms, at least three possible changes could happen in the brain: (i) The intervention could 'repair' all or a subset of the brain abnormalities preexisting in these individuals, (ii) the intervention could result in compensatory mechanisms that do not alter the preexisting brain abnormalities, (iii) the intervention might not alter the brain. Through hypothesis-2a, we tested whether CBT causes HRF changes in any region of the brain, irrespective of whether it was compensatory or repair. Through hypothesis-2b we tested whether the intervention could 'repair' preexisting HRF abnormalities in OCD. We tested these hypotheses using whole-brain voxel-level HRF data estimated from resting-state fMRI.

METHODS

Participants

Forty-four individuals with a DSM-IV diagnosis of OCD were recruited from local clinics and the community, along with 25 healthy controls (HC). Informed consent was obtained from all participants. The UCLA Institutional Review Board approved the study. A board-certified psychiatrist (JDF) having clinical experience with OCD populations confirmed the diagnoses upon performing comprehensive evaluations. The *ADIS-IV Mini* was employed for primary OCD and comorbid diagnoses. Eligible individuals scored ≥16 on the Yale-Brown Obsessive Compulsive Scale (YBOCS) [61]. See Supplemental Information S1 for detailed information, including inclusion/exclusion criteria, comorbidities and medications.

FMRI data acquisition and pre-processing

Whole-brain BOLD fMRI resting-state data was obtained using a Siemens Trio 3T scanner (Siemens Medical Solutions USA Inc., Malvern, Pennsylvania) using a 12-channel phased-array head coil. Scan parameters were as follows: T2* weighted EPI; acquisition time = 7 minutes; TR/TE=2000/25ms; flip angle=78°; matrix=64×64; field of view= 195 mm; in-plane voxel size=3×3 mm^2; slice thickness=3 mm; total interleaved slices=35. A high resolution (1-mm isotropic) T1 weighted MPRAGE sequence was also used to collect anatomical data for coregistration. Data was obtained on two different occasions for each participant (see Fig.3 for time-flow diagram): (i) OCD participants, pre- and post- 4 weeks intensive CBT, and (ii) HCs, sessions 1 and 2 separated by 4 weeks, to form an appropriate control for the pre- and post-treatment OCD scans. The exposure and response prevention (ERP)-based intensive CBT treatment involved 90-minute one-on-one sessions 5 days a week for 4 weeks, was conducted by two licensed therapists, and was focused on improving OCD symptoms (for details see [50]). Twenty-one of the OCD patients received an

additional fMRI scan 4-weeks prior to the CBT, with no treatment activity during the time between this and the pre-treatment MRI scans (allowed assessing the effect of time without interventional treatment).

All the fMRI pre-processing steps were performed using Statistical Parametric Mapping (SPM8, http://www.fil.ion.ucl.ac.uk/spm), as follows. The first four volumes were discarded to allow participants to adapt to scanner noise and to obtain signal equilibrium. The raw EPI images were realigned, coregistered, normalized to the 2mm MNI space (affine transformation), and smoothed with an 8-mm Gaussian kernel. We used the artifact detection tool (ART) (http://www.nitrc.org/projects/artifact_detect) to calculate head motion. For each participant, head motion along each of the three translational and three rotational directions was computed. The "aggregate" motion calculated by ART was a composite from all six head-motion parameters. The exclusion criteria were any relative head motion exceeding 2 mm along the translational axes or 2 degrees angular motion along the rotational axes. Based on these criteria, no participant was excluded. No significant difference was observed in aggregate motion between groups (mean±SD; HCs: 0.15±0.06 mm, OCD: 0.13±0.07mm; range; HCs: [0.06,0.93], OCD: [0.08, 0.89]; P=0.23). The CompCor method [62] (implemented in SPM) was employed to regress-out motion, CSF and white matter signals. The resulting whole-brain 3D+time fMRI data was used in further analysis.

Deconvolution

We next performed deconvolution to extract the HRF parameters from the BOLD fMRI data. Employing the method of Wu et al. [63], the 3D+time data were deconvolved across time at every voxel to get the latent neural time series and the HRF parameters. Several recent studies have utilized this technique (for example [8] [20] [64] [22] [65] [66] [67]). The validity of this technique has been demonstrated using simulations by Wu et. al. [63], Tagliazuchi et. al. [68] as well as Rangaprakash et. al. [19]. The deconvolution procedure is "blind" because we have access to the fMRI timeseries (one variable) only, from which the technique estimates both the latent neural timeseries and the HRF. Briefly, the technique [63] models resting-state fMRI as event-related timeseries with randomly occurring point-process events [69] (since the participant performs no designed task in resting-state), and then evaluates voxel-wise HRFs using Wiener deconvolution [70]. Deconvolution estimated one HRF for the entire time series at every voxel. Like in previous studies [65] [8], a temporal mask with aggregate head motion <0.3 mm was added to avoid pseudo point-process events induced by motion artifacts [71]. The measure of deconvolution quality (mean squared error between original and fitted data) was assessed and found to be not statistically significant between the groups. The deconvolution code is available at [72]. All data analysis was performed on the Matlab® R2015a platform.

HRF analysis

Deconvolution estimated the HRF time series at each voxel in every participant for each scan session. The HRF was characterized by three parameters – response height (RH), time-to-peak (TTP), and full-width at half-max (FWHM), as described. RH, a measure of HRF amplitude, is conceptually similar, although not identical, to BOLD activation; higher RH results from elevated excitatory or decreased inhibitory neurotransmitters, from increased

CBF or vasodilation [3], all of which are also associated with higher activation [31]. While higher BOLD signal could result from either larger RH or increased latent neural activity or both, the RH allows us to investigate physiological factors *other* than neural firing, such as excitatory/inhibitory neurotransmitter balance, which might contribute towards a larger BOLD response. For instance, glutamate acts on NMDA receptors, causing vasodilation [47] and increasing the CBF [45], which in turn results in elevated HRF RH [46]. TTP measures the latency of the BOLD response, while FWHM is related to the duration of the BOLD response, both of which are less likely to be directly associated, if at all, with activation. Importantly, RH, TTP and FWHM are not correlated across the brain [73] [74], suggesting that they carry unique information and may measure distinct underlying phenomena.

We first performed a 2-way ANOVA with group and time as factors (HC vs OCD and session-1 vs session-2), separately for each HRF parameter ($p<0.05$, cluster-level and FDR thresholded, controlled for age, education and head-motion). We additionally performed a similar secondary ANOVA analysis to compare changes that occurred over 4 weeks in the OCD group that received CBT to the OCD-waitlist subset group that did not receive CBT but was scanned twice, separated by 4 weeks. Group and time were the factors, wherein the 'group' factor was CBT vs. no CBT in OCD and time was pre- 4 weeks and post- 4 weeks. Compared to the previous ANOVA, this comparison was not confounded by the possibility that the HRF in OCD individuals might change differently over 4 weeks of no treatment compared to the effects of the same passage of time in HC. Tests for statistical significance were performed separately on each of the three parameters to obtain voxel-specific differences in HRF parameters (two-sample T-test, $p<0.05$, cluster-level and FDR thresholded, controlled for age, education and head-motion). Cluster thresholding was performed through permutation testing. Additionally, we corrected for the multiple comparisons of probing three HRF parameters (Bonferroni's method). We tested each of our hypotheses as follows.

(1) Hypothesis-1 (*HRF is sensitive to neuropathology: OCD individuals will exhibit HRF aberrations compared to HC at baseline*): whole-brain statistics (T-test) Session-1 HC vs. pre-CBT OCD, separately for RH, TTP and FWHM. As a secondary analysis, we compared the HRF against fractional amplitude of low frequency fluctuations (fALFF), which is another regional resting-state fMRI measure known to be sensitive to pathology [75] [76] (Supplemental Information S4).

(2) Hypothesis-2 (*HRF is sensitive to treatment, and predictive of treatment response*): (2a) *In OCD, CBT will change the shape of the HRF post-treatment compared to pre-treatment*: whole-brain statistics (T-test) post-CBT OCD vs. pre-CBT OCD, separately for RH, TTP and FWHM. As a control analysis, we measured HRF differences in HCs between two scans spaced 4 weeks apart, as well as in the OCD-waitlist subset group between the two scans spaced by 4 weeks of no treatment.

(2b) *A subset of the pre-CBT HRF aberrations in OCD will return to normalcy post-CBT*: In 2a, we tested for whole-brain changes in HRF with treatment, that is, we were probing the question, "what HRF changes did treatment cause in the entire brain?" In 2b, we probed the question, "which of the abnormal regions in pre-CBT OCD, as tested in *hypothesis-1*,

showed change post-treatment?" To test this, we first assessed the group×time interaction, followed by T-tests where we limited our statistical analysis to only those regions that were found significant with *hypothesis-1* (impairments in pre-CBT OCD), and performed statistics within those regions: OCD post-treatment vs. pre-treatment, separately for RH, TTP and FWHM. Probing this provided us those regions that exhibited significantly abnormal HRF in pre-CBT OCD *and* significantly changed HRF after treatment (i.e., abnormal regions that "normalized" with treatment). Among the regions identified, we confirmed that there was no significant difference between the HRF values in post-CBT OCD compared to Session-2 HC, to ascertain that the HRF "normalized" (that is, not significantly different than healthy controls) after treatment. Such observations allowed identification of pathological brain regions in OCD that were "corrected" by CBT.

(2c) *Change in HRF with treatment will be associated with corresponding changes in OCD symptom severity*: Using linear regression, we probed the association between the percentage change in HRF parameters with treatment (each parameter separately) across each of the identified significant regions (*hypothesis-2a*) and the percentage change in YBOCS with treatment.

(2d) *Pre-treatment HRF parameters would predict treatment outcome in OCD*: We performed supervised machine learning classification with HRF data to achieve two objectives: (i) determining the ability of OCD pre-treatment HRF values in predicting treatment response, and (ii) identifying those brain regions that possessed the highest predictive ability. Statistical relationships (such as association) between imaging measures and clinical variables do not necessarily imply that they have predictive ability [77]; that is, they may not be able to predict at the individual-subject level with reasonable accuracy. Since association does not necessarily imply prediction, it is also true that imaging features that exhibit both statistical association and predictive ability assume more importance. This analysis helped in the identification of such important imaging features that were both predictive of and associated with treatment outcome. Treatment responders were defined (based on expert consensus [78]) as those exhibiting 35% or more reduction in YBOCS with treatment. Binary supervised classification was performed with the pre-treatment HRF parameters for distinguishing between treatment responders and non-responders. To simultaneously achieve the two objectives, we employed a feature elimination based machine learning technique called recursive cluster elimination based support vector machine classifier (RCE-SVM) [79] (linear kernel), which recursively eliminates input features that contribute poorly towards classification, finally retaining only those features that are responsible for the best prediction (for details see [8] [80]). The inputs to the classifier were only those HRF parameters from voxels that exhibited significant difference in OCD pre-treatment compared to HCs (i.e. findings with *hypothesis-1*). This was done to restrict the features to only those voxels that were relevant to OCD pathology. This did not bias the classification since treatment response was not taken into consideration while performing OCD pre-treatment vs. HC analysis. In the case of this study, since the pathological regions were also found to "normalize" with treatment, this would have inflated the performance (although not circularly) [81] because voxels not relevant to OCD pathology (that were not included) would be expected to be less discriminatory features. Training set comprised of 80% of the participants, with the remaining forming the testing

set. The algorithm was initiated with 40 clusters [79] in the first RCE step, and least performing 20% of clusters were discarded in each successive RCE step until only one cluster remained, giving us the best classification accuracy. Six-fold cross-validation was performed to split the data in each iteration into training and testing sets with the ratio 5:1, and the algorithm was executed for 100 repetitive loops (in order to account for different splits) to give a total of 600 independent classification cycles. Recent studies have shown that the choice of these parameters provides reliable results [8] [67]. This technique simultaneously provided us the voxel-level top-predictive HRF parameters that best predicted treatment response at baseline, and the classification accuracy provided by those features (although, it is important to note that this is a multivariate analysis, such that all remaining features contribute to the prediction). Lastly, results from statistical analysis, associations with clinical variables and top-predictors from machine learning were assembled together to draw broader conclusions from this study.

RESULTS

Demographics and clinical variables

Demographics and clinical information for both HC and OCD groups appear in Table 1. There were no significant group differences in sex, age or education.

Effects of pathology and time

There was a general, consistent pattern of shorter, quicker and narrower HRFs in OCD pre-treatment compared to HC at baseline, and relatively taller, longer and broader HRFs in OCD post-treatment compared to pre-treatment, implying that lower RH, TTP and FWHM are associated with OCD pathology and their increase is associated with CBT treatment. With the 2-way ANOVA, we found a significant main effect of group (F=9.69±1.05, P=0.002±0.001) (Supplemental Information S5– Fig.S2a–c) and a significant main effect of time (F=8.65±0.95, P=0.004±0.001) (Fig.S2d–f) with all 3 HRF parameters, and a significant group×time interaction (F=6.89±0.83, P=0.008±0.001) with RH and TTP (Fig.S3). With the secondary ANOVA analysis between OCD and OCD-waitlist subset groups across time, we found a significant main effect of group (F=8.42±0.99, P=0.006±0.001) and a significant main effect of time (F=8.54±0.98, P=0.005±0.001) with all 3 HRF parameters, and a significant group×time interaction (F=7.21±0.91, P=0.007±0.002) with RH and TTP. In the following paragraphs, we will present pairwise group comparisons with RH and TTP in order to test specific hypotheses (pairwise tests with FWHM were not performed since it did not exhibit group×time interaction; refer to Fig.S2c and Fig.S2f for FWHM ANOVA results).

HRF sensitivity to OCD pathology

With hypothesis-1 (*HRF is sensitive to pathology*), shorter RH was found in pre-CBT OCD than in Session-1 (baseline) HC regionally in right thalamus (mostly in the pulvinar), right caudate head, right cuneus, and bilateral superior parietal cortex (Fig.4a) (T=3.23±0.31, effect size: Cohen's d=0.78±0.08). Quicker TTP was found in right caudate tail and left supplementary motor area (Fig.4b) (T=3.23±0.30, Cohen's d=0.78±0.09). Also refer to Table 2 for T-statistics, volumes and centroid coordinates of these results.

HRF sensitivity to CBT treatment

For the OCD post-treatment vs. pre-treatment comparison (*hypothesis-2a*), increases in RH were found in bilateral precuneus (Fig.4c) (T=3.03±0.27, Cohen's *d*=0.73±0.09), and increases in TTP was found in the right caudate tail (Fig.4d) (T=2.89±0.29, Cohen's *d*=0.70±0.07). Also refer to Table 2 for T-statistics, volumes and centroid coordinates of these results. Part of the caudate tail exhibited baseline abnormalities (*hypothesis-1*) as well as change with treatment (*hypothesis-2a*), that is, there was a non-zero intersection between the two statistical maps in this region. There were no significant HRF differences between Session-1 HC and Session-2 HC (P>0.05), nor between the two scans of OCD-waitlist subset group without intervening treatment (P>0.05).

Next, regarding hypothesis-2b (*subset of OCD pre-CBT HRF aberrations would return to normalcy post-CBT*), we found evidence that RH in the caudate head and TTP in the caudate tail, which were abnormal in pre-CBT OCD, changed after CBT, and did not statistically differ (P>0.05, uncorrected) from the values in HC session-2 (the regions identifiable in Figs. 4a and 4b, and marked in **bold** in Table 2). These two regions were abnormal in OCD before treatment and normalized towards the HC pattern after treatment. There was no significant difference in these voxels between post-CBT OCD and Session-2 HC at 4 weeks. Given that RH in caudate head and TTP in caudate tail were among the most important findings, we illustrate the corresponding HRFs in these regions (averaged across subjects) and boxplots in Fig.5. We also separately compared medicated (N=15) and unmedicated (N=29) OCD participants, as well as the entire OCD sample (N=44) compared with unmedicated OCD participants, both at the voxel-level across the whole-brain, and found no significant differences in RH, TTP, or FWHM in either pre-CBT or post-CBT HRF parameters (highest T-value = 1.21, lowest P-value = 0.23) (see Supplemental Information S6). Additionally, we found that depressive symptoms did not have an impact on our results (see Supplemental Information S7). In summary, we found lower value of HRF parameters in OCD pre-treatment compared to HC, and an increase in HRF parameters after treatment that appeared to "normalize" towards the HC pattern.

HRF association with OCD severity

In accordance with hypothesis-2c (*HRF change with treatment will be associated with YBOCS change*), we found significant negative association between (Fig.6a) percentage change in HRF RH and percentage change in OCD severity (YBOCS) with CBT treatment (R=−0.44, R^2=0.19, P=0.0028) in the caudate head region. Larger increases in HRF RH with treatment were associated with larger decreases in OCD severity. We also assessed various quality measures of regression to find that the regression did not violate the homoscedasticity assumption (P=0.20, Engle's ARCH test), the residuals were uniformly distributed (P=0.73, Chi-square goodness-of-fit test) and no influential observations were found (P<0.008, leave-one-out regressions) (see Supplemental Information S8).

Prediction of treatment outcome

For the machine learning analysis, the inputs to the classifier were, as mentioned earlier, only those HRF parameters from *hypothesis-1* findings (Session-1 HC vs pre-CBT OCD) (Fig.4a–b), which restricted the features to only those relevant to OCD pathology at

baseline. We found that pre-treatment HRF values predicted treatment outcome with 86.41% accuracy (significantly greater than chance, $P<10^{-50}$) (sensitivity=92.88%, specificity=77.06%). Among the 44 OCD participants, 26 were responders and 18 were non-responders; we found the balanced classification accuracy to be 84.97%. The final top-predictive features that resulted in this accuracy were the RH from 24 voxels in the right caudate head and 11 voxels in the right thalamus, and TTP from 14 voxels in the right caudate tail.

In addition, we performed a null-test using HRF data from different regions, specifically those which had the least difference between pre-CBT OCD and Session-1 HC (largest p-values, $P>0.8$). Using the same number of input features in an identical machine learning framework, we observed an accuracy of 58.84%, which was close to chance accuracy. This assures that our accuracy of 86.41% arose primarily from relevant HRF values, which was significantly higher than the null-test accuracy ($P<10^{-50}$).

In addition to pre-CBT HRF predicting post-treatment OCD severity, both also exhibited a statistical association. We found a significant negative association between pre-CBT HRF RH in the caudate head and OCD severity (YBOCS) after treatment ($R=-0.48$, $R^2=0.23$, $P=0.001$) (Fig.6b). Higher HRF RH before treatment was associated with lower OCD severity after treatment. We also assessed various quality measures of regression to find that the regression did not violate the homoscedasticity assumption ($P=0.76$, Engle's ARCH test), the residuals were uniformly distributed ($P=0.14$, Chi-square goodness-of-fit test) and no influential observations were found ($P<0.0076$, leave-one-out regressions) (see Supplemental Information S8).

RH in the caudate head, in summary, was abnormal before treatment, changed with treatment, predicted post-treatment OCD severity, was associated with change in OCD severity with treatment, and possessed high predictive ability for treatment outcome. TTP in the caudate tail was abnormal before treatment, changed with treatment, and possessed high predictive ability for treatment outcome.

DISCUSSION

The goal of this study was to assess the relevance of HRF shape to brain functioning, OCD pathology and interventional CBT treatment. This goal was motivated by prior research that supports the idea that the HRF carries mechanistically pertinent information related to neuronal activity, in spite of prevailing views of the HRF as an undesirable low pass filter of neural activity and HRF variability as a confound of no interest. We hypothesized that the HRF is sensitive to OCD pathology and CBT treatment.

We found evidence in support of our hypotheses. We found that the HRF is abnormal in OCD (*hypothesis-1*, Fig.4a–c). We found that CBT causes HRF changes in OCD (*hypothesis-2a*, Fig.4d–f), and that a subset of the pre-CBT HRF aberrations in OCD "normalize" (change towards the pattern in HC) post-treatment (*hypothesis-2b*). We found that, with treatment, the change in RH was associated with the change in OCD severity (*hypothesis-2c*, Fig.6a). Further, pre-treatment RH predicted post-treatment OCD severity

(Fig.6b). Finally, the HRF could predict treatment response with 86.4% accuracy (*hypothesis-2d*). These results suggest that the HRF is sensitive to brain pathology in OCD and can detect changes with CBT treatment. We discuss each of these findings in detail.

HRF aberrations in OCD

HRF was sensitive to OCD pathology. *RH abnormalities* in OCD were observed in parts of the conventional CSTC OCD circuit [82] [83]. The caudate head, which is part of the striatum, is pivotal in habit learning and procedural memory [84], which are associated with core OCD symptoms [85] [86]. Moreover, thalamic impairment has been found to result in aberrant orbitofrontal function [85], ultimately exacerbating OCD symptoms. There is evidence that, specifically, the right striato-thalamic circuit may be primarily impaired in OCD [87], corroborating our findings. While most studies report increased activation of the caudate head and thalamus [85] [86], we observed decreased RH in OCD. Recent studies, however, have reported decreased activation [88] and magnitude of local resting-state fMRI measures in OCD, especially in the CSTC circuit, for example with regional homogeneity (ReHo) [89] and fALFF [90]. Another well-designed event-related symptom provocation study [91] found deactivation in the caudate while the provocations were perceived intense by OCD participants, implying that hyporesponse in the caudate is possible under certain task conditions. Better understanding of the HRF parameters from future studies might reveal further insights. It is notable that we did not find RH differences in any prefrontal regions, including any in the CSTC circuit; in this way, our findings differ qualitatively from some previous conventional fMRI studies, many of which identify prefrontal abnormalities [82] [85] [90] [89] [92] [93] [94] [95] [96] [97]. In summary, we identified HRF abnormalities in subcortical regions largely implicated in OCD pathophysiology in earlier conventional fMRI studies.

Abnormal lateral parietal function has also been identified in several OCD studies, especially those investigating the fronto-parietal network in OCD [98] [99]. Such studies have interpreted impaired superior parietal function as possibly reflecting the inability of persons with OCD to disengage from everyday tasks requiring external attention [98]. It is interesting to note that the pulvinar (the thalamic region identified in this study) is known to have functional relationships with visual regions (also identified in this study) [100]. Taken together, RH results share some similarities with findings from conventional fMRI analyses from previous studies yet do not completely overlap, suggesting that these differing approaches reflect partially distinct neural processes.

CBF, measured using single photon emission computed tomography (SPECT) in [32], has been found to be abnormal in OCD in basal ganglia and the occipital cortex, regions identified in the current study as having abnormal HRF RH in OCD at baseline. CBF has also been found to be reduced in the caudate following CBT treatment in OCD patients [60] (measured using positron emission tomography [PET] and SPECT), corroborating our HRF RH findings. These interesting similarities between CBF and HRF RH must be studied further not only in the context of OCD but also other pathological conditions. FMRI acquisition (and thus HRF estimated from it) has certain advantages over direct imaging of CBF using PET, SPECT or perfusion MRI, therefore a direct link between PET/SPECT/

perfusion measures of CBF and fMRI measure of HRF shape would suggest additional utility of HRF measures.

TTP and FWHM findings diverged from RH findings, and were not in regions commonly identified in previous, conventional OCD fMRI studies. Specifically, there were TTP abnormalities in the caudate tail, not often associated with OCD. We reiterate that TTP measures the latency of the BOLD signal, which is not captured by conventional activation or functional connectivity modeling, hence this finding might indicate previously underexplored mechanisms of OCD pathophysiology. The caudate tail is involved in learning [101] [102], which is a reflection of neural flexibility. Impaired learning could be associated with cognitive rigidity. Huntington's disease, for example, which involves physical rigidity and diminished capacity for motor control and ultimately cognitive rigidity in later stages [103], begins in the caudate tail and spreads from there [104]. OCD is also characterized by a degree of cognitive rigidity, and diminished capacity for behavioral control over motor functions (although not directly a loss over motor control as in Huntington's). The caudate tail may have an important role in OCD origins and pathophysiology. To date, fMRI studies have not reported impairments in activation or functional connectivity of the caudate tail in OCD. This aspect deserves further investigation in future studies.

HRF changes with CBT treatment

The HRF was sensitive to a 4-week intensive CBT treatment. While we noticed lower HRF parameters in pre-CBT OCD compared to HCs, post-treatment OCD exhibited higher HRF parameters compared to pre-treatment, implying that the HRF parameters changed in the healthy direction with treatment. RH changes were observed in bilateral precuneus, previously shown to exhibit changes with CBT treatment [57] as part of the default-mode network. TTP changes were observed in the caudate tail.

Among those regions that exhibited abnormalities in OCD before treatment, we observed significant change in RH with treatment in the caudate head and TTP in the caudate tail (*hypothesis-1*). In these regions, there were no significant differences between post-CBT OCD and Session-2 HC, implying that they were abnormal before treatment and were "normalized" with treatment. As a control comparison, there were no HRF differences in HCs between two scans spaced 4 weeks apart, as well as in the OCD-waitlist subset group between the two scans spaced by 4 weeks of no treatment. Additionally, RH in the caudate head before treatment predicted OCD severity after treatment, and change in RH with treatment in this region was significantly associated with change in OCD severity. The direction of these associations was as expected, with higher pre-treatment RH predicting lower OCD severity after treatment, and larger increase in RH with treatment corresponding with larger reduction in OCD severity. Banca et al. [91] found mean caudate head deactivation during single, strong symptom provocation exposure events. Following from this finding, our observation of RH in the caudate head being abnormally low prior to treatment and changing with treatment (tracking with reduction in YBOCS) could reflect the possibility that as those with OCD improve, when their symptoms are provoked the caudate would show less deactivation. These findings highlight the behavioral relevance of HRF

parameters, specifically the RH in the OCD population. They also highlight the importance of RH in the caudate head, a region repeatedly shown to have abnormal activity in OCD [105] [86], which was abnormal in OCD before treatment, changed after treatment, was associated with reduction in OCD severity with treatment and could predict post-treatment OCD severity. Put together, these results lend credence to our hypothesis that the HRF is sensitive to brain pathology and interventional treatment. While we have tested this proposition in the OCD population, future studies are necessary to explore HRF as a marker of pathology and treatment effects in other clinical populations. To this effect, the authors have so far explored the HRF as a marker of PTSD [20] and autism [21] pathology.

From the machine learning analysis, we found that pre-treatment HRF data could predict the outcome of the intensive 4-week CBT treatment with 86.4% accuracy. More importantly, the algorithm determined, in a data driven way, that the RH in the caudate head and thalamus, and TTP in the caudate tail were most salient in predicting treatment outcome even before the treatment was started.

Implications of our findings

With these findings, we suggest that the resting-state HRF RH in the caudate head and TTP in the caudate tail are important for OCD pathology and treatment outcome. RH in the caudate head was abnormal before treatment, it changed after treatment, it predicted post-treatment OCD severity, it was associated with change in OCD severity with treatment and lastly it possessed high ability in predicting treatment outcome. TTP in the caudate tail was abnormal before treatment, it changed after treatment and lastly it possessed high ability in predicting treatment outcome. Although findings from animal [106] and human [107] spectroscopic studies have been inconclusive with regard to neurometabolic abnormalities in OCD, we observed HRF changes in OCD. Given the relationship between HRF and neurometabolites described earlier, our conjecture to explain this disparity is that spectroscopic studies focus on specific neurometabolites while the HRF is an aggregate (and maybe more robust) measure of multiple neurovascular factors including neuronal activity, multiple neurometabolites and neurovascular coupling. In summary, this study provides evidence for the utility of the shape of the HRF derived from resting-state fMRI as a marker of brain function, pathology and treatment outcome.

In our recent study involving the same participant cohorts [50], network connectivity appeared to be less sensitive to baseline abnormalities in OCD, compared with detecting changes from CBT. Therefore, connectivity likely identified networks whose changes were compensatory in nature rather than representing “normalization” of underlying pathology. On the contrary, from the current study, the HRF appeared to possibly be more sensitive to baseline abnormalities than to changes with CBT, based simply on the observation that there were a larger number of regions and voxels that were significantly different in the former case (113 vs. 47 voxels; refer to Table 2). At the very least, this provides evidence that the nature of information obtained from the HRF shape is different compared to that obtained by functional connectivity analysis of BOLD time series. Nonetheless, the common feature between the connectivity and HRF findings was that there was little overlap between the regions or networks showing baseline differences (OCD pre-treatment vs. HC) and those

showing changes with CBT. This further supports the premise that CBT treatment for OCD, at least in the short-term activates largely compensatory mechanisms that are distinct from the core neural mechanisms involved in OCD pathology.

The HRF parameters (especially TTP and FWHM) are qualitatively different from conventional fMRI-derived measures, and hence might provide novel insights unavailable through conventional approaches. FMRI BOLD activation quantifies the relative amplitude of brain activity, but not the latency/sluggishness of BOLD response, which is related to how quickly the corresponding brain regions are being recruited. This is measured by TTP and FWHM, which, as discussed earlier, is modulated by local neurochemistry. While higher BOLD signal could result from either larger RH or increased latent neural activity or both, looking exclusively at RH allows us to investigate physiological factors other than neural firing, such as excitatory/inhibitory neurotransmitter balance, which might contribute towards a larger BOLD response. Functional connectivity, which quantifies coactivation, also does not directly measure latency. We invite researchers to probe these aspects further as additional research is required to confirm these specific observations. The unique perspective provided by HRF does not merely arise from which brain regions are implicated with HRF differences. Rather, they arise from the fact that activation, connectivity and HRF changes tell different things about the underlying mechanism. For example, caudate head is implicated in OCD through all of these three approaches (across this and other studies), which tells us that OCD involves altered post-synaptic activity (fMRI activation), altered neural synchrony with other regions (connectivity) as well as altered neurovascular coupling (HRF) in this region. This study was not designed to resolve which of these alterations cause which others; in fact, studies in the same participants, rather than across studies with different participants, are necessary to directly compare these methods of analyses. However, we demonstrate the HRF to be a window into investigating pathology- and treatment-related changes, possibly in the same (or different) regions as those implicated by activation and connectivity, that may rely on mechanisms that are distinct from those underlying activation and connectivity.

Likewise, further research is necessary to assess the interrelationship between the HRF parameters. These parameters are generally uncorrelated, although lower RH might possibly be associated with larger TTP or FWHM. However, a recent study found lower RH in aging and in those with vascular risk but no altered TTP or FWHM in those cases [108]. In our study, the majority of regions showing RH changes were not associated with TTP or FWHM changes. Within our data, we did not observe significant correlation across subjects between whole-brain HRF parameters (see Supplemental Information S9). Despite these observations, based on the underlying biophysics, there is sufficient grounds to hypothesize a direct relationship between the HRF parameters in healthy adults, as well as a shift in that relationship in brain-related illnesses. These questions are open to investigation.

We performed supplemental analyses, which were not central to this study's hypotheses, yet provide some early groundwork for investigation in future studies. First, we assessed the relevance of HRF to normal brain function, with the specific case of primary motor function (Supplemental Information S2). The difference in RH between the right and left primary motor cortices was associated with percentage right handedness. Future studies focusing

primarily on the healthy brain are needed to examine possible relationships of the HRF shape with other aspects of normal functioning. Second, we assessed the longitudinal reliability of HRF. While connectivity dynamics can change in seconds, the HRF is reasonably stable over time scales of minutes to hours [1], and perhaps even days/weeks. Our supplemental analysis suggested that the HC and OCD-waitlist subset groups (scanned twice with no intervening treatment) showed significant, moderate longitudinal reliability between HRF parameters obtained 4 weeks apart (see Supplemental Information S3). Taking our findings forward in future studies, stability is a necessary condition for use of imaging parameters as potential biomarkers of disease [109]. Our results suggest that the HRF has promise on this front, although future studies are needed to replicate these results. Third, results using fALFF showed highest similarity with RH results, with classification accuracy significantly greater than chance although not as high as with the HRF parameters (Supplemental Information S4). Future studies could assess the predictive ability of the HRF parameters in comparison with other fMRI measures using a larger sample, to assess the suitability of the HRF parameters as biomarkers, perhaps augmenting other conventional fMRI measures.

There are several implications of these findings, taken together. A general methodological implication is that the HRF is an fMRI-derived regional measure that is sensitive to brain function, pathology and treatment outcome. Future investigations could probe the fundamental relationships between the HRF and other fMRI measures, as well as the common and distinguishing characteristics of each of the three HRF parameters. Future studies could also utilize this technique to derive novel mechanistic insights into healthy brain functioning as well as psychiatric and neurologic disorders. In addition, there are more specific clinical implications for the OCD participant sample that we studied. Abnormal RH in the caudate head, complementing previous neuroimaging studies' finding of abnormal glucose metabolism, BOLD activity, and regional volumes [105] [86], helps to further characterize pathology of this region and circuits involving this region, in OCD. In addition, the observation that RH in the caudate head and TTP in the caudate tail "normalize" with treatment suggests that this marker of pathology may actually be remediated by CBT. These regions are also clinically relevant in that their HRF parameters could predict treatment outcome at pre-treatment baseline. Taken together, the most prominent set of findings from these analyses that reflect OCD pathophysiology, effects of treatment, and prediction of treatment response involve HRF measures in the caudate nucleus. RH in the caudate head and TTP in the caudate tail were abnormal before treatment, changed after treatment, and possessed strong ability to predict treatment outcome. Additionally, RH in the caudate head predicted post-treatment OCD severity and was associated with treatment-related change in OCD severity. These findings, if replicated, have direct implications for OCD diagnosis, prognosis, tracking treatment progress and mechanistic understanding of the underlying neurobiology of OCD.

This study has several limitations. (i) Our sample size was modest. (ii) Our OCD cohort included some individuals on medication, which could have influenced the findings; yet, no significant HRF differences were found (within the regions identified in this study) between medicated and unmedicated individuals, nor between the combined cohort used in this study and unmedicated individuals (see Supplemental Information S6). (iii) As typical for fMRI

processing, deconvolution of BOLD fMRI only provides analytically best indirect estimates of the latent neuronal time series and the ground-truth HRF, while making assumptions during the estimation given that events are not defined *a priori* in resting-state fMRI (additional discussion points are provided in Supplemental Information S10). The HRF-deconvolution utilizes a heuristic scheme to estimate neural events from the time series and relies upon temporal shift-invariant linearity of the HRF. While this approach has been validated using simulations in previous studies [63] [68] [19], we believe that future experimental studies may provide a firm grounding for the deconvolution approach. Specifically, in order to know exactly how the estimated data fits the ground truth, one would have to invasively measure the hemodynamic response to a single neural event while simultaneously acquiring fMRI data [27] [110] [111]. Alternatively, event-related task fMRI could be employed [74] (however, see Supplemental Information S10 for issues in using event-related task fMRI versus using resting-state fMRI for estimating the HRF). While such an endeavor is outside the scope of this paper, such future studies are needed in order to make stronger conclusions about links between HRF morphology and pathology. (iv) We tested multiple hypotheses in this study and compared across multiple groups and longitudinal time points. As such, we performed a high number of statistical tests, despite corrections. This renders the study still rather exploratory. (v) By performing a 6-fold cross-validation, only $5/6^{th}$ of the participants (i.e. 37 OCD participants, randomly different ones in each iteration) were used as training data during machine learning classification. A smaller sample size is often associated with higher likelihood of over-fitting [112]. Our sample size (N_{OCD}=44) was not large enough for us to use some participants for feature selection (using training-testing as done in this study) and the remaining participants as a separate hold-out validation set for assessing model performance. We performed feature selection and model validation using the entire sample, although cross-validation was performed. Future studies with larger samples would enable a left-out validation sample to be used. (vi) This study was based on resting-state fMRI, which does not necessarily generalize to HRF changes during controlled task experiments [113]. (vi) Unlike RH, the temporal resolution of fMRI matters significantly more for accurate estimation of TTP and FWHM, since the resolution of these measures is limited by the repetition time (TR) of fMRI acquisition. At TR = 2 seconds, our study had relatively low temporal resolution. This could result in an inability to detect true group differences as well as associations of TTP and FWHM with clinical variables (if they exist). We suggest readers to view negative observations regarding TTP and FWHM in this light; we recommend future researchers to study this problem with HRF parameters obtained from data with better (sub-second) temporal resolution. Newer multiband pulse-sequences with higher temporal resolution may mitigate this HRF temporal resolution limitation.

Supplementary Material

Refer to Web version on PubMed Central for supplementary material.

Acknowledgements:

We acknowledge Michelle Massi and Natalie Abrahami for their role in providing cognitive-behavioral therapy treatment for the participants with obsessive-compulsive disorder in this study.

Funding: This study was supported by US National Institutes of Mental Health (NIMH) grant R01 MH085900 (to Drs. Feusner and O'Neill).

REFERENCES

[1]. Handwerker DA, Ollinger JM and D'Esposito M, "Variation of BOLD hemodynamic responses across subjects and brain regions and their effects on statistical analyses," Neuroimage, vol. 21, no. 4, pp. 1639–51, 2004. [PubMed: 15050587]

[2]. Biessmann F, Murayama Y, Logothetis N, Müller K and Meinecke F, "Improved decoding of neural activity from fMRI signals using non-separable spatiotemporal deconvolutions," Neuroimage, vol. 61, no. 4, pp. 1031–42, 2012. [PubMed: 22537598]

[3]. Aguirre GK, Zarahn E and D'esposito M, "The variability of human, BOLD hemodynamic responses," Neuroimage, vol. 8, no. 4, pp. 360–9, 1998. [PubMed: 9811554]

[4]. Buxton R, "Introduction to Functional Magnetic Resonance Imaging: Principles and Techniques," Energy, vol. 24, no. 2, pp. xi, 523, 2002.

[5]. Levin J, Ross M, Mendelson J, Kaufman M, Lange N, Maas L, Mello N, Cohen B and Renshaw P, "Reduction in BOLD fMRI response to primary visual stimulation following alcohol ingestion," Psychiatry Research, vol. 82, no. 3, p. 135–46, 1998. [PubMed: 9754438]

[6]. Noseworthy M, Alfonsi J and Bells S, "Attenuation of brain BOLD response following lipid ingestion," Human Brain Mapping, vol. 20, no. 2, p. 116–121, 2003. [PubMed: 14505337]

[7]. Friston K, Harrison L and Penny W, "Dynamic causal modelling," Neuroimage, vol. 19, no. 4, pp. 1273–302, 2013.

[8]. Rangaprakash D, Deshpande G, Daniel T, Goodman A, Robinson J, Salibi N, Katz J, Denney T and Dretsch M, "Compromised Hippocampus-Striatum Pathway as a Potential Imaging Biomarker of Mild Traumatic Brain Injury and Posttraumatic Stress Disorder," Human Brain Mapping, vol. 38, no. 6, pp. 2843–64, 2017. [PubMed: 28295837]

[9]. Deshpande G, Sathian K and Hu X, "Effect of hemodynamic variability on Granger causality analysis of fMRI," Neuroimage, vol. 52, no. 3, pp. 884–96, 2010. [PubMed: 20004248]

[10]. Lacey S, Stilla R, Sreenivasan K, Deshpande G and Sathian K, "Spatial imagery in haptic shape perception," Neuropsychologia, vol. 60, pp. 144–158, 2014. [PubMed: 25017050]

[11]. Feng C, Deshpande G, Liu C, Gu R, Luo Y-J and Krueger F, "Diffusion of responsibility attenuates altruistic punishment: A functional magnetic resonance imaging effective connectivity study," Human Brain Mapping, vol. 37, no. 2, pp. 663–77, 2015. [PubMed: 26608776]

[12]. Libero L, DeRamus T, Lahti A, Deshpande G and Kana R, "Multimodal neuroimaging based classification of autism spectrum disorder using anatomical, neurochemical, and white matter correlates," Cortex, vol. 66, pp. 46–59, 2015. [PubMed: 25797658]

[13]. Grant M, Wood K, Sreenivasan K, Wheelock M, White D, Thomas J, Knight D and Deshpande G, "Influence of early life stress on intra- and extra-amygdaloid causal connectivity," Neuropsychopharmacology, vol. 40, no. 7, pp. 1782–93, 2015. [PubMed: 25630572]

[14]. Hampstead B, Khoshnoodi M, Yan W, Deshpande G and Sathian K, "Patterns of effective connectivity between memory encoding and retrieval differ between patients with mild cognitive impairment and healthy older adults," NeuroImage, vol. 124, no. A, pp. 997–1008, 2016. [PubMed: 26458520]

[15]. Sreenivasan K, Havlicek M and Deshpande G, "Non-parametric hemodynamic deconvolution of fMRI using homomorphic filtering," IEEE Transactions on Medical Imaging, vol. 34, no. 5, pp. 1155–63, 2015. [PubMed: 25531878]

[16]. Ryali S, Supekar K, Chen T and Menon V, "Multivariate dynamical systems models for estimating causal interactions in fMRI," Neuroimage, vol. 54, no. 2, pp. 807–23, 2011. [PubMed: 20884354]

[17]. Ryali S, Chen T, Supekar K, Tu T, Kochalka J, Cai W and Menon V, "Multivariate dynamical systems-based estimation of causal brain interactions in fMRI: Group-level validation using benchmark data, neurophysiological models and human connectome project data," Journal of Neuroscience Methods, vol. 268, pp. 142–53, 2016. [PubMed: 27015792]

[18]. Ryali S, Shih Y, Chen T, Kochalka J, Albaugh D, Fang Z, Supekar K, Lee J and Menon V, "Combining optogenetic stimulation and fMRI to validate a multivariate dynamical systems model for estimating causal brain interactions," Neuroimage, vol. 132, pp. 398–405, 2016. [PubMed: 26934644]

[19]. Rangaprakash D, Wu G-R, Marinazzo D, Hu X and Deshpande G, "Hemodynamic response function (HRF) variability confounds resting-state fMRI functional connectivity," Magnetic Resonance in Medicine, p. in press, 2018.

[20]. Rangaprakash D, Dretsch MN, Yan W, Katz JS, Denney TS and Deshpande G, "Hemodynamic variability in soldiers with trauma: Implications for functional MRI connectivity studies," NeuroImage: Clinical, vol. 16, pp. 409–417, 2017. [PubMed: 28879082]

[21]. Yan W, Rangaprakash D and Deshpande G, "Aberrant hemodynamic responses in Autism: Implications for resting state fMRI functional connectivity studies," NeuroImage: Clinical, vol. 19, pp. 320–330, 2018. [PubMed: 30013915]

[22]. Rangaprakash D, Dretsch MN, Yan W, Katz JS, Denney TS and Deshpande G, "Hemodynamic response function parameters obtained from resting-state functional MRI data in soldiers with trauma," Data in Brief, vol. 14, pp. 558–562, 2017. [PubMed: 28861454]

[23]. Yan W, Rangaprakash D and Deshpande G, "Hemodynamic response function parameters obtained from resting state BOLD fMRI data in subjects with Autism Spectrum Disorder and matched healthy controls," Data in Brief, vol. 14, pp. 558–562, 2017. [PubMed: 28861454]

[24]. Rangaprakash D, Dretsch MN, Yan W, Katz JS, Denney TS and Deshpande G, "Hemodynamic variability in soldiers with trauma: Implications for functional MRI connectivity studies," NeuroImage: Clinical, p. in press, 2017.

[25]. Deshpande G, Sathian K and Hu X, "Effect of hemodynamic variability on Granger causality analysis of fMRI," Neuroimage, vol. 52, no. 3, pp. 884–96, 2010. [PubMed: 20004248]

[26]. Handwerker DA, Gonzalez-Castillo J, D'Esposito M and Bandettini PA, "The continuing challenge of understanding and modeling hemodynamic variation in fMRI," Neuroimage, vol. 62, no. 2, pp. 1017–23, 2012. [PubMed: 22366081]

[27]. David O, Guillemain I, Saillet S, Reyt S, Deransart S, Segebarth C and Depaulis A, "Identifying neural drivers with functional MRI: an electrophysiological validation," PLoS Biology, vol. 23, no. 6, pp. 2683–97, 2008.

[28]. Havlicek M, Friston KJ, Jan J, Brazdil M and Calhoun VD, "Dynamic modeling of neuronal responses in fMRI using cubature Kalman filtering," Neuroimage, vol. 56, no. 4, pp. 2109–28, 2011. [PubMed: 21396454]

[29]. Havlicek M, Jan J, Brazdil M and Calhoun V, "Dynamic Granger causality based on Kalman filter for evaluation of functional network connectivity in fMRI data," Neuroimage, vol. 53, no. 1, pp. 65–77, 2010. [PubMed: 20561919]

[30]. Wang Y, David O, Hu X and Deshpande G, "Can Patel's τ accurately estimate directionality of connections in brain networks from fMRI?," Magnetic Resonance in Medicine, vol. 78, no. 5, pp. 2003–2010, 2017. [PubMed: 28090665]

[31]. Buxton R, Wong E and Frank L, "Dynamics of blood flow and oxygenation changes during brain activation: the balloon model," Magnetic Resonance in Medicine, vol. 39, no. 6, pp. 855–64, 1998. [PubMed: 9621908]

[32]. Wen S, Cheng M, Cheng M, Yue J, Li J and Xie L, "Neurocognitive dysfunction and regional cerebral blood flow in medically naive patients with obsessive-compulsive disorder," Developmental Neuropsychology, vol. 39, no. 1, pp. 37–50, 2014. [PubMed: 24405183]

[33]. Liu F, Zhuo C and Yu C, "Altered Cerebral Blood Flow Covariance Network in Schizophrenia," Frontiers in Neuroscience, vol. 10, p. 308, 2016. [PubMed: 27445677]

[34]. Grieder M, Crinelli R, Jann K, Federspiel A, Wirth M, Koenig T, Stein M, Wahlund L and Dierks T, "Correlation between topographic N400 anomalies and reduced cerebral blood flow in the anterior temporal lobes of patients with dementia," Journal of Alzheimer's Disease, vol. 36, no. 4, pp. 711–31, 2013.

[35]. Hamilton J, Farmer M, Fogelman P and Gotlib I, "Depressive rumination, the Default-Mode Network, and the dark matter of clinical neuroscience," Biological Psychiatry, vol. 78, pp. 224–230, 2015. [PubMed: 25861700]

[36]. Zürcher N, Bhanot A, McDougle C and Hooker J, “A systematic review of molecular imaging (PET and SPECT) in autism spectrum disorder: Current state and future research opportunities,” Neuroscience and Biobehavioral Reviews, vol. 52, p. 56–73, 2015. [PubMed: 25684726]

[37]. Goozée R, Handley R, Kempton M and Dazzan P, “A systematic review and meta-analysis of the effects of antipsychotic medications on regional cerebral blood flow (rCBF) in schizophrenia: Association with response to treatment,” Neuroscience and Biobehavioral Reviews, vol. 43, p. 118–136, 2014. [PubMed: 24690578]

[38]. Halani S, Kwinta J, Golestani A, Khatamian Y and Chen J, “Comparing cerebrovascular reactivity measured using BOLD and cerebral blood flow MRI: The effect of basal vascular tension on vasodilatory and vasoconstrictive reactivity,” Neuroimage, vol. 110, pp. 110–123, 2015. [PubMed: 25655446]

[39]. Kim J and Ress D, “Arterial impulse model for the BOLD response to brief neural activation,” Neuroimage, vol. 124(Pt A), pp. 394–408, 2016. [PubMed: 26363350]

[40]. Golestani A, Wei L and Chen J, “Quantitative mapping of cerebrovascular reactivity using resting-state BOLD fMRI: Validation in healthy adults,” Neuroimage, vol. 138, pp. 147–163, 2016. [PubMed: 27177763]

[41]. Len TK and Neary JP, “Cerebrovascular pathophysiology following mild traumatic brain injury,” Clinical Psychology and Functional Imaging, vol. 31, no. 2, pp. 85–93, 2011.

[42]. Lemke H, de Castro A, Schlattmann P, Heuser I and Neu P, “Cerebrovascular reactivity over time-course - from major depressive episode to remission,” Journal of Psychiatry Research, vol. 44, no. 3, pp. 132–136, 2010.

[43]. Reynell C and Harris J, “The BOLD signal and neurovascular coupling in autism,” Developmental Cognitive Neuroscience, vol. 6, pp. 72–79, 2013. [PubMed: 23917518]

[44]. Duarte J, Pereira J, Quendera B, Raimundo M, Moreno C, Gomes L, Carrilho F and Castelo-Branco M, “Early disrupted neurovascular coupling and changed event level hemodynamic response function in type 2 diabetes: an fMRI study,” Journal of Cerebral Blood Flow and Metabolism, vol. 35, no. 10, pp. 1671–1680, 2015. [PubMed: 26058698]

[45]. Buzsáki G, Kaila K and Raichle M, “Inhibition and brain work,” Neuron, vol. 56, no. 5, pp. 771–83, 2007. [PubMed: 18054855]

[46]. Brown GG, Eyler Zorrilla LT, Georgy B, Kindermann SS, Wong EC and Buxton RB, “BOLD and perfusion response to finger-thumb apposition after acetazolamide administration: differential relationship to global perfusion,” Journal of Cerebral Blood Flow and Metabolism, vol. 23, no. 7, pp. 829–37, 2003. [PubMed: 12843786]

[47]. Busija DW, Bari F, Domoki F and Louis T, “Mechanisms involved in the cerebrovascular dilator effects of N-methyl-d-aspartate in cerebral cortex,” Brain Research Reviews, vol. 56, no. 1, p. 89–100, 2007. [PubMed: 17716743]

[48]. Muthukumaraswamy SD, Evans CJ, Edden RA, Wise RG and Singh KD, “Individual variability in the shape and amplitude of the BOLD-HRF correlates with endogenous GABAergic inhibition,” Human Brain Mapping, vol. 33, no. 2, pp. 455–65, 2012. [PubMed: 21416560]

[49]. Cohen Z, Bonvento G, Lacombe P and Hamel E, “Serotonin in the regulation of brain microcirculation,” Progress in Neurobiology, vol. 50, no. 4, pp. 335–62, 1996. [PubMed: 9004349]

[50]. Moody T, Morfini F, Cheng G, Sheen C, Tadayonnejad R, Reggente N, O’Neill J and Feusner J, “Mechanisms of cognitive-behavioral therapy for obsessive-compulsive disorder involve robust and extensive increases in brain network connectivity,” Translational Psychiatry, vol. 7, no. 9, p. el230, 2017.

[51]. O’Neill J and Feusner J, “Cognitive-behavioral therapy for obsessive-compulsive disorder: access to treatment, prediction of long-term outcome with neuroimaging,” Psychology Research and Behavior Management, vol. 8, pp. 211–223, 2015. [PubMed: 26229514]

[52]. Olatunji B, Ferreira-Garcia R, Caseras X, Fullana M, Wooderson S, Speckens A, Lawrence N, Giampietro V, Brammer M, Phillips M, Fontenelle L and Mataix-Cols D, “Predicting response to cognitive behavioral therapy in contamination-based obsessive-compulsive disorder from functional magnetic resonance imaging,” Psychological Medicine, vol. 44, no. 10, pp. 2125–37, 2014. [PubMed: 24229474]

[53]. O'Neill J, Lai T, Sheen C, Salgari G, Ly R, Armstrong C, Chang S, Levitt J, Salamon N, Alger J and Feusner J, "Cingulate and thalamic metabolites in obsessive-compulsive disorder," Psychiatry Research, vol. 254, pp. 34–40, 2016. [PubMed: 27317876]

[54]. Saxena S, Gorbis E, O'Neill J, Baker S, Mandelkern M, Maidment K, Chang S, Salamon N, Brody A, Schwartz J and London E, "Rapid effects of brief intensive cognitive-behavioral therapy on brain glucose metabolism in obsessive-compulsive disorder," Molecular Psychiatry, vol. 14, no. 2, pp. 197–205, 2009. [PubMed: 18180761]

[55]. Apostolova I, Block S, Buchert R, Osen B, Conradi M, Tabrizian S, Gensichen S, Schroder-Hartwig K, Fricke S, Rufer M, Weiss A, Hand I, Clausen M and Obrocki J, "Effects of behavioral therapy or pharmacotherapy on brain glucose metabolism in subjects with obsessive-compulsive disorder as assessed by brain FDG PET," Psychiatry Research: Neuroimaging, vol. 184, p. 105–116, 2010. [PubMed: 20947317]

[56]. Nakatani E, Nakgawa A, Ohara Y, Goto S, Uozumi N, Iwakiri M, Yamamoto Y, Motomura K, Iikura Y and Yamagami T, "Effects of behavior therapy on regional cerebral blood flow in obsessive-compulsive disorder," Psychiatry Research: Neuroimaging, vol. 124, p. 113–120, 2003.

[57]. Yang X-Y, Sun J, Luo J, Zhong Z-X, Li P, Yao S-M, Xiong H-F, Huang F-F and Li Z-J, "Regional homogeneity of spontaneous brain activity in adult patients with obsessive–compulsive disorder before and after cognitive behavioural therapy," Journal of Affective Disorders, vol. 188, p. 243–251, 2015. [PubMed: 26378734]

[58]. Zurowski B, Kordon A, Weber-Fahr W, Voderholzer U, Kuelz A, Freyer T, Wahl K, Biichel C and Hohagen F, "Relevance of orbitofrontal neurochemistry for the outcome of cognitive-behavioural therapy in patients with obsessive-compulsive disorder," European Archives of Psychiatry and Clinical Neuroscience, vol. 262, no. 7, pp. 617–624, 2012. [PubMed: 22427151]

[59]. Yamanishi T, Nakaaki S, Omori I, Hashimoto N, Shinagawa Y, Hongo J, Horikoshi M, Tohyama J, Akechi T, Soma T, Iidaka T and Furukawa T, "Changes after behavior therapy among responsive and nonresponsive patients with obsessive-compulsive disorder," Psychiatry Research: Neuroimaging, vol. 172, p. 242–250, 2009.

[60]. van der Straten A, Denys D and van Wingen G, "Impact of treatment on resting cerebral blood flow and metabolism in obsessive compulsive disorder: a meta-analysis," Scientific Reports, vol. 7, no. 1, p. 17464, 2017. [PubMed: 29234089]

[61]. Goodman W, Price L, Rasmussen S, Mazure C, Fleischmann R, Hill C, Heninger G and Charney D, "The Yale-Brown Obsessive Compulsive Scale. I. Development, use, and reliability," Archives of General Psychiatry, vol. 46, no. 11, pp. 1006–11, 1989. [PubMed: 2684084]

[62]. Behzadi Y, Restom K, Liau J and Liu T, "A component based noise correction method (CompCor) for BOLD and perfusion based fMRI," Neuroimage, vol. 37, no. 1, pp. 90–101, 2007. [PubMed: 17560126]

[63]. Wu G, Liao W, Stramaglia S, Ding J, Chen H and Marinazzo D, "A blind deconvolution approach to recover effective connectivity brain networks from resting state fMRI data," Medical Image Analysis, vol. 17, no. 3, pp. 365–374, 2013. [PubMed: 23422254]

[64]. Boly M, Sasai S, Gosseries O, Oizumi M, Casali A, Massimini M and Tononi G, "Stimulus set meaningfulness and neurophysiological differentiation: a functional magnetic resonance imaging study," PLoS One, vol. 10, no. 5, p. e0125337, 2015. [PubMed: 25970444]

[65]. Amico E, Gomez F, Di Perri C, Vanhaudenhuyse A, Lesenfants D, Boveroux P, Bonhomme V, Brichant JF, Marinazzo D and Laureys S, "Posterior cingulate cortex-related co-activation patterns: a resting state FMRI study in propofol-induced loss of consciousness," PLoS One, vol. 9, no. 6, p. e100012, 2014. [PubMed: 24979748]

[66]. Lamichhane B, Adhikari BM, Brosnan SF and Dhamala M, "The neural basis of perceived unfairness in economic exchanges," Brain Connectivity, vol. 4, no. 8, pp. 619–30, 2014. [PubMed: 25090304]

[67]. Rangaprakash D, Dretsch M, Venkatraman A, Katz J, Denney T and Deshpande G, "Identifying Disease Foci from Static and Dynamic Effective Connectivity Networks: Illustration in Soldiers with Trauma," Human Brain Mapping, vol. 39, no. 1, pp. 264–287, 2018. [PubMed: 29058357]

[68]. Tagliazucchi E, Balenzuela P, Fraiman D and Chialvo D, "Criticality in large-scale brain fMRI dynamics unveiled by a novel point process analysis," Frontiers in Physiology, p. 3:15, 2012.

[69]. Saad ZS, Gotts SJ, Murphy K, Chen G, Jo HJ, Martin A and Cox RW, “Trouble at rest: how correlation patterns and group differences become distorted after global signal regression,” Brain Connectivity, vol. 2, no. 1, pp. 25–32, 2012. [PubMed: 22432927]

[70]. Glover G, “Deconvolution of impulse response in event-related BOLD fMRI,” Neuroimage, vol. 9, no. 4, pp. 416–29, 1999. [PubMed: 10191170]

[71]. Power JD, Schlaggar BL and Petersen SE, “Recent progress and outstanding issues in motion correction in resting state fMRI,” Neuroimage, vol. 105, pp. 536–51, 2015. [PubMed: 25462692]

[72]. Marinazzo D, “Code for HRF blind deconvolution,” 2013. [Online]. Available: http://users.ugent.be/~dmarinaz/HRF_deconvolution.html. [Accessed Sept 2016].

[73]. Miezin F, Maccotta L, Ollinger J, Petersen S and Buckner R, “Characterizing the hemodynamic response: effects of presentation rate, sampling procedure, and the possibility of ordering brain activity based on relative timing,” Neuroimage, vol. 11(6 Pt 1), pp. 735–759, 2000. [PubMed: 10860799]

[74]. Taylor A, Kim J and Ress D, “Characterization of the hemodynamic response function across the majority of human cerebral cortex,” Neuroimage, vol. 173, pp. 322–331, 2018. [PubMed: 29501554]

[75]. Tadayonnejad R, Yang S, Kumar A and Ajilore O, “Clinical, cognitive, and functional connectivity correlations of resting-state intrinsic brain activity alterations in unmedicated depression,” Journal of Affective Disorders, vol. 172, pp. 241–50, 2015. [PubMed: 25451423]

[76]. Zuo X, Di Martino A, Kelly C, Shehzad Z, Gee D, Klein D, Castellanos F, Biswal B and Milham M, “The oscillating brain: complex and reliable,” Neuroimage, vol. 49, no. 2, pp. 1432–45, 2010. [PubMed: 19782143]

[77]. Arbabshirani M, Plis S, Sui J and Calhoun V, “Single subject prediction of brain disorders in neuroimaging: Promises and pitfalls,” NeuroImage, vol. 145, no. Pt B, pp. 137–165, 2017. [PubMed: 27012503]

[78]. Mataix-Cols D, Fernández L de la Cruz A Nordsletten F Lenhard K Isomura and Simpson H, “Towards an international expert consensus for defining treatment response, remission, recovery and relapse in obsessive-compulsive disorder,” World Psychiatry, vol. 15, no. 1, pp. 80–1, 2016. [PubMed: 26833615]

[79]. Deshpande G, Li Z, Santhanam P, Coles CLM, Hamann S and Hu X, “Recursive cluster elimination based support vector machine for disease state prediction using resting state functional and effective brain connectivity,” PLoS One, vol. 5, no. 12, p. e14277, 2010. [PubMed: 21151556]

[80]. Deshpande G, Li Z, Santhanam P, Coles C, Lynch M, Hamann S and Hu X, “Recursive cluster elimination based support vector machine for disease state prediction using resting state functional and effective brain connectivity,” PLoS One, vol. 5, no. 12, p. e14277, 2010. [PubMed: 21151556]

[81]. Craddock R, Holtzheimer III P, Hu X and Mayberg H, “Disease State Prediction From Resting State Functional Connectivity,” Magnetic Resonance in Medicine, vol. 62, no. 6, pp. 1619–28, 2009. [PubMed: 19859933]

[82]. Saxena S and Rauch S, “Functional neuroimaging and the neuroanatomy of obsessive-compulsive disorder,” The Psychiatric Clinics of North America, vol. 23, no. 3, pp. 563–586, 2000. [PubMed: 10986728]

[83]. van den Heuvel O, van Wingen G, Soriano-Mas C, Alonso P, Chamberlain S, Nakamae T, Denys D, Goudriaan A and Veltman D, “Brain circuitry of compulsivity,” Eur Neuropsychopharmacol., vol. 26, no. 5, pp. 810–27, 2016. [PubMed: 26711687]

[84]. Morris L, Baek K and Voon V, “Distinct cortico-striatal connections with subthalamic nucleus underlie facets of compulsivity,” Cortex, vol. 88, pp. 143–150, 2017. [PubMed: 28103527]

[85]. Maia T, Cooney R and Peterson B, “The neural bases of obsessive-compulsive disorder in children and adults,” Development and Psychopathology, vol. 20, no. 4, pp. 1251–83, 2008. [PubMed: 18838041]

[86]. Rasgon A, Lee W, Leibu E, Laird A, Glahn D, Goodman W and Frangou S, “Neural correlates of affective and non-affective cognition in obsessive compulsive disorder: A meta-analysis of functional imaging studies,” Eur Psychiatry., vol. 46, pp. 25–32, 2017. [PubMed: 28992533]

[87]. Rauch S, Whalen P, Savage C, Curran T, Kendrick A, Brown H, Bush G, Breiter H and Rosen B, "Striatal recruitment during an implicit sequence learning task as measured by functional magnetic resonance imaging," Human Brain Mapping, vol. 5, no. 2, pp. 124–32, 1997. [PubMed: 10096417]

[88]. Tang W, Zhu Q, Gong X, Zhu C, Wang Y and Chen S, "Cortico-striato-thalamo-cortical circuit abnormalities in obsessive-compulsive disorder: A voxel-based morphometric and fMRI study of the whole brain," Behav Brain Res., vol. 313, pp. 17–22, 2016. [PubMed: 27388149]

[89]. Niu Q, Yang L, Song X, Chu C, Liu H, Zhang L, Li Y, Zhang X, Cheng J and Li Y, "Abnormal resting-state brain activities in patients with first-episode obsessive-compulsive disorder," Neuropsychiatric Disease and Treatment, vol. 13, pp. 507–513, 2017. [PubMed: 28243104]

[90]. Qiu L, Fu X, Wang S, Tang Q, Chen X, Cheng L, Zhang F, Zhou Z and Tian L, "Abnormal regional spontaneous neuronal activity associated with symptom severity in treatment-naive patients with obsessive-compulsive disorder revealed by resting-state functional MRI," Neuroscience Letters, vol. 640, pp. 99–104, 2017. [PubMed: 28104431]

[91]. Banca P, Voon V, Vestergaard M, Philipiak G, Almeida I, Pocinho F, Relvas J and Castelo-Branco M, "Imbalance in habitual versus goal directed neural systems during symptom provocation in obsessive-compulsive disorder," Brain, vol. 138, no. Pt 3, pp. 798–811, 2015. [PubMed: 25567322]

[92]. Maltby N, Tolin D, Worhunsky P, O'Keefe T and Kiehl K, "Dysfunctional action monitoring hyperactivates frontal-striatal circuits in obsessive-compulsive disorder: an event-related fMRI study," Neuroimage, vol. 24, pp. 495–503, 2005. [PubMed: 15627591]

[93]. Milad M, Furtak S, Greenberg J, Keshaviah A, Im J, Falkenstein M, Jenike M, Rauch S and Wilhelm S, "Deficits in conditioned fear extinction in obsessive-compulsive disorder and neurobiological changes in the fear circuit," JAMA Psychiatry, vol. 70, no. 6, pp. 608–618, 2013. [PubMed: 23740049]

[94]. Beucke J, Sepulcre J, Talukdar T, Linnman C, Zschenderlein K, Endrass T, Kaufmann C and Kathmann N, "Abnormally high degree connectivity of the orbitofrontal cortex in obsessive-compulsive disorder," JAMA Psychiatry, vol. 70, no. 6, pp. 619–629, 2013. [PubMed: 23740050]

[95]. Anticevic A, Hu S, Zhang S, Savic A, Billingslea E, Wasylink S, Repovs G, Cole M, Bednarski S, Krystal J, Bloch M, Li C-S and Pittenger C, "Global resting-state functional magnetic resonance imaging analysis identifies frontal cortex, striatal, and cerebellar dysconnectivity in obsessive-compulsive disorder," Biological Psychiatry, vol. 75, p. 595–605, 2014. [PubMed: 24314349]

[96]. Cheng Y, Xu J, Nie B, Luo C, Yang T, Li H, Lu J, Xu L, Shan B and Xu X, "Abnormal resting-state activities and functional connectivities of the anterior and the posterior cortexes in medication-naive patients with obsessive-compulsive disorder," PLoS One, vol. 8, no. 6, p. e67478, 2013. [PubMed: 23840714]

[97]. Hou J-M, Zhao M, Zhang W, Song L-H, Wu W-J, Wang J, Zhou D-Q, Xie B, He M, Guo J-W, Qu W and Li H-T, "Resting-state functional connectivity abnormalities in patients with obsessive-compulsive disorder and their healthy first-degree relatives," Journal of Psychiatry and Neuroscience, vol. 39, no. 5, p. 304–11, 2014. [PubMed: 24866415]

[98]. Stem E, Fitzgerald K, Welsh R, Abelson J and Taylor S, "Resting-state functional connectivity between fronto-parietal and default mode networks in obsessive-compulsive disorder," PLoS One, vol. 7, no. 5, p. e36356, 2012. [PubMed: 22570705]

[99]. Gürsel D, Avram M, Sorg C, Brandi F and Koch K, "Frontoparietal areas link impairments of large-scale intrinsic brain networks with aberrant fronto-striatal interactions in OCD: a meta-analysis of resting-state functional connectivity," Neurosci Biobehav Rev., vol. 87, pp. 151–160, 2018. [PubMed: 29410103]

[100]. Arcaro M, Pinsk M and Kastner S, "The Anatomical and Functional Organization of the Human Visual Pulvinar," Journal of Neuroscience, vol. 35, no. 27, pp. 9848–71, 2015. [PubMed: 26156987]

[101]. Seger C and Cincotta C, "The roles of the caudate nucleus in human classification learning," Journal of Neuroscience, vol. 25, no. 11, pp. 2941–51, 2005. [PubMed: 15772354]

[102]. Kim H, Ghazizadeh A and Hikosaka O, “Separate groups of dopamine neurons innervate caudate head and tail encoding flexible and stable value memories,” Front Neuroanat, vol. 8, p. 120, 2014. [PubMed: 25400553]

[103]. Johnson A and Paulsen J, Understanding behavior in Huntington’s Disease: A guide for professionals, Lovecky D and Tarapata K, Eds., New York: Huntington’s Disease Society of America, 2014.

[104]. Aylward E, Sparks B, Field K, Yallapragada V, Shpritz B, Rosenblatt A and et al., “Onset and rate of striatal atrophy in preclinical Huntington disease,” Neurology, vol. 63, no. 1, pp. 66–72, 2004. [PubMed: 15249612]

[105]. Menzies L, Chamberlain S, Laird A, Thelen S, Sahakian B and Bullmore E, “Integrating evidence from neuroimaging and neuropsychological studies of obsessive-compulsive disorder: the orbitofronto-striatal model revisited,” Neurosci Biobehav Rev., vol. 32, no. 3, pp. 525–49, 2008. [PubMed: 18061263]

[106]. Mintzopoulos D, Gillis T, Robertson H, Dalia T, Feng G, Rauch S and Kaufman M, “Striatal magnetic resonance spectroscopy abnormalities in young adult SAPAP3 knockout mice,” Biol Psychiatry Cogn Neurosci Neuroimaging., vol. 1, no. 1, pp. 39–48, 2016. [PubMed: 26858992]

[107]. Brennan B, Rauch S, Jensen J and Pope H, “A critical review of magnetic resonance spectroscopy studies of obsessive-compulsive disorder,” Biol Psychiatry, vol. 73, no. 1, pp. 24–31,2013. [PubMed: 22831979]

[108]. McDonough I, Bender A, Patihis L, Stinson E, Letang S and Miller W, “The Trouble Interpreting fMRI Studies in Populations with Cerebrovascular Risk: The Use of a Subject-Specific Hemodynamic Response Function in a Study of Age, Vascular Risk, and Memory,” bioRxiv, p. 512343, 2019.

[109]. Raemaekers M, du Plessis S, Ramsey N, Weusten J and Vink M, “Test-retest variability underlying fMRI measurements,” Nenroimage, vol. 60, no. 1, pp. 717–27, 2012.

[110]. Wang Y, Katwal S, Rogers B, Gore J and Deshpande G, “Experimental Validation of Dynamic Granger Causality for Inferring Stimulus-evoked Sub-100ms Timing Differences from fMRI,” IEEE Tram Neural Syst Rehabil Eng., p. in press, 2016.

[111]. Wang Y, David O, Hu X and Deshpande G, “Can Patel’s τ accurately estimate directionality of connections in brain networks from fMRI?,” Magnetic Resonance in Medicine, vol. 78, no. 5, pp. 2003–10, 2017. [PubMed: 28090665]

[112]. Lanka P, Rangaprakash D, Dretsch M, Katz J, Denney T and Deshpande G, “Supervised machine learning for diagnostic classification from large-scale neuroimaging datasets,” Brain Imaging Behav., p. in press, 2019.

[113]. Chen J and Glover G, “BOLD fractional contribution to resting-state functional connectivity above 0.1 Hz,” Neuroimage, vol. 107, p. 207–18, 2015. [PubMed: 25497686]

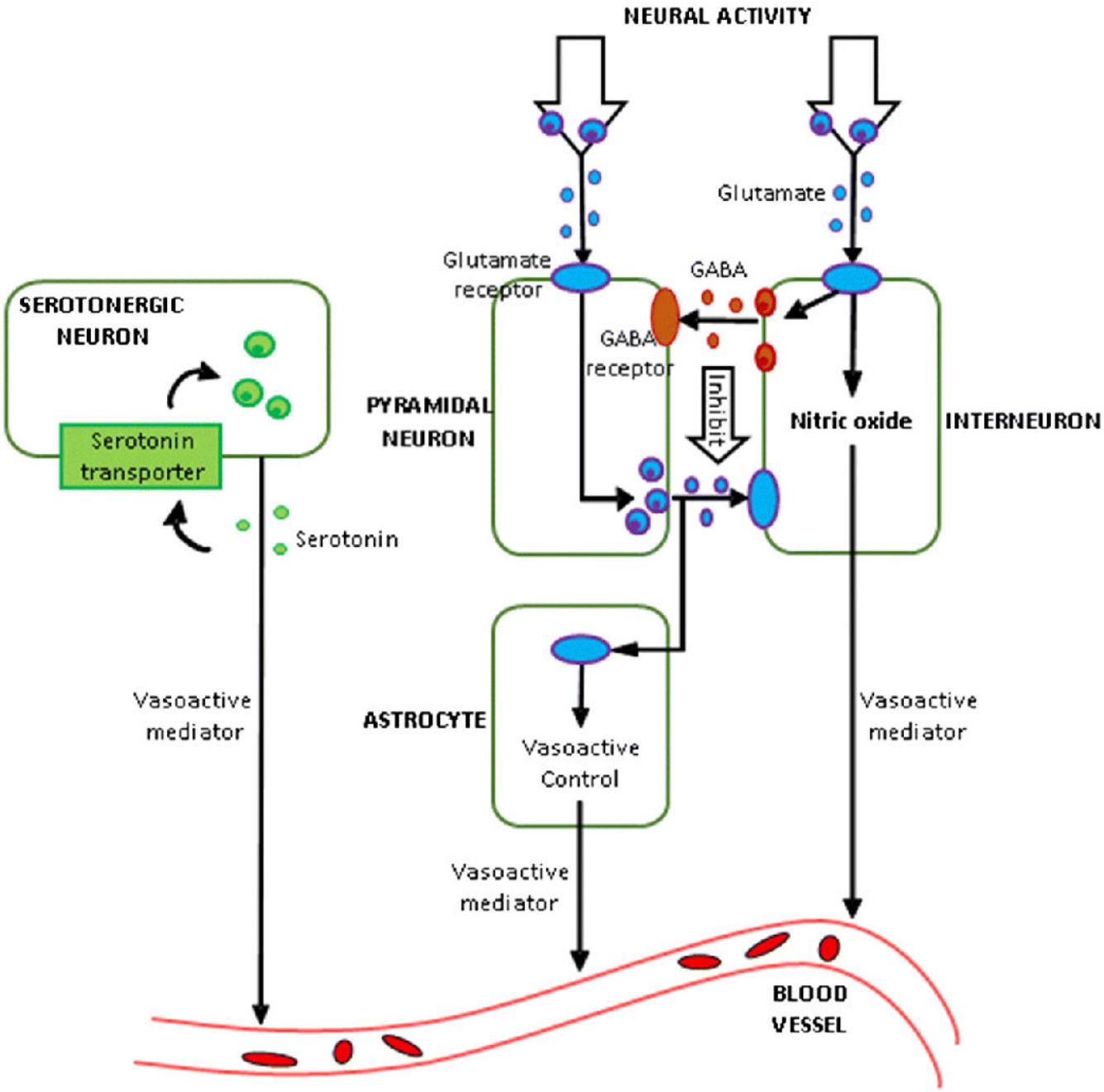

Fig.1.

A putative biophysical model of neurovascular coupling illustrating neural signaling mechanisms which might control the shape of the HRF (adapted from [43]).

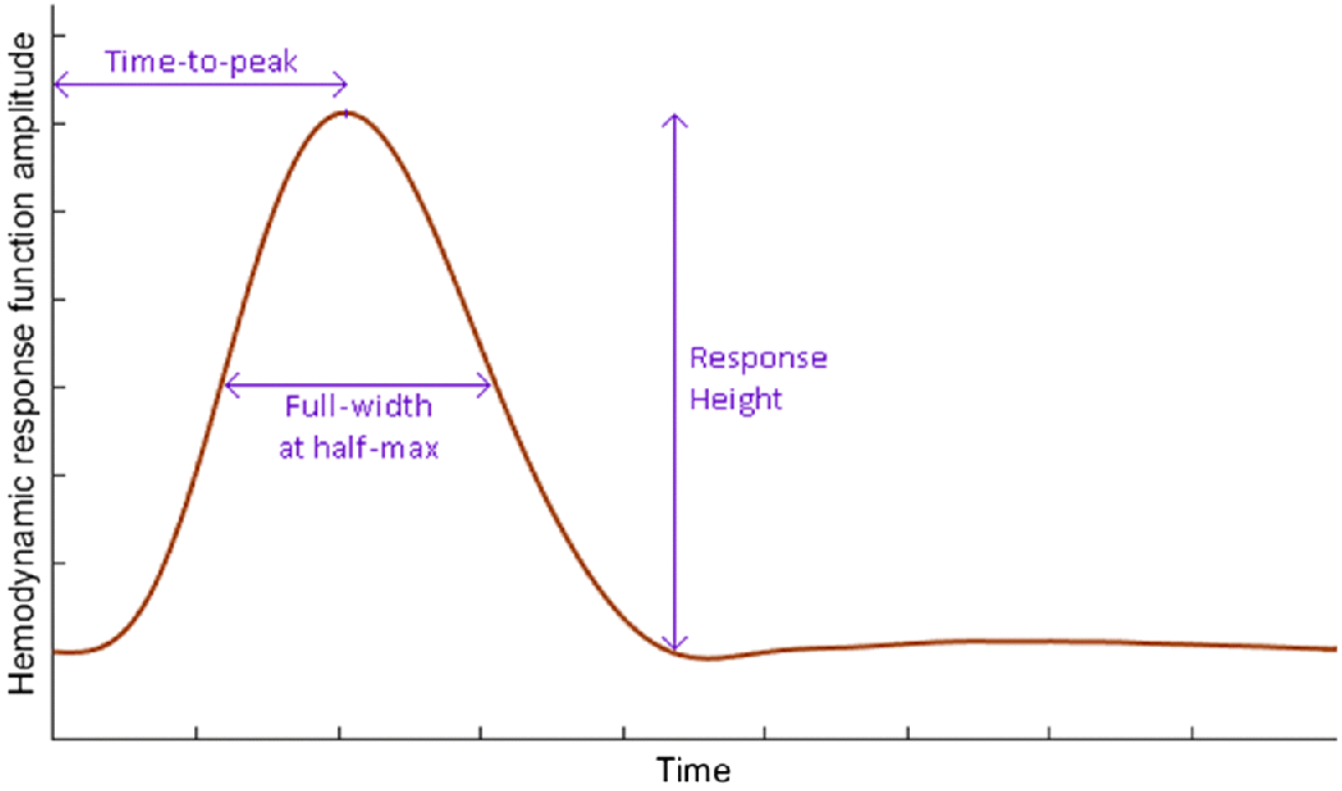

Fig.2.

The hemodynamic response function (HRF) with its three parameters: response height, time-to-peak and full-width at half maximum.

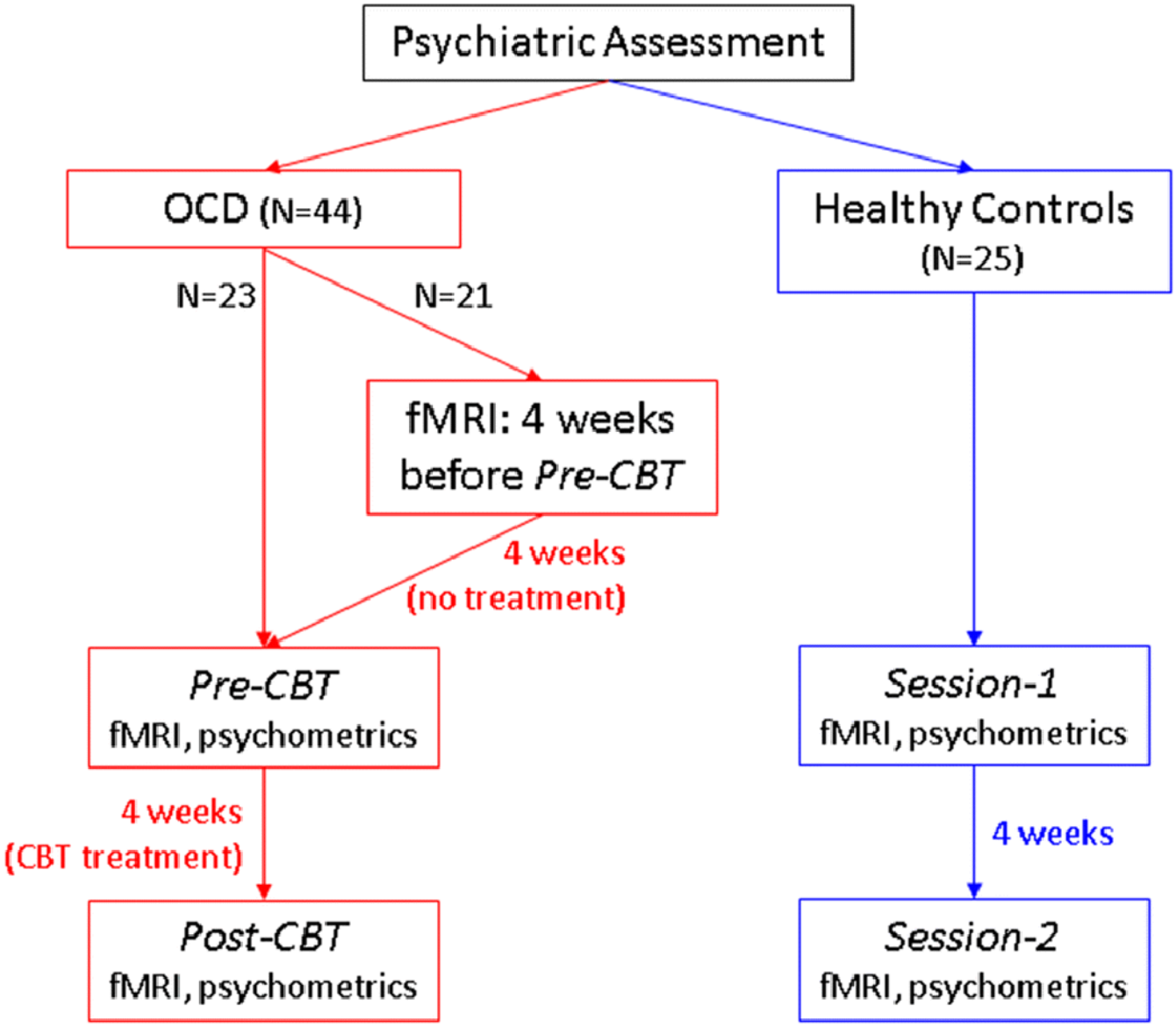

Fig.3.
Data acquisition time-flow diagram

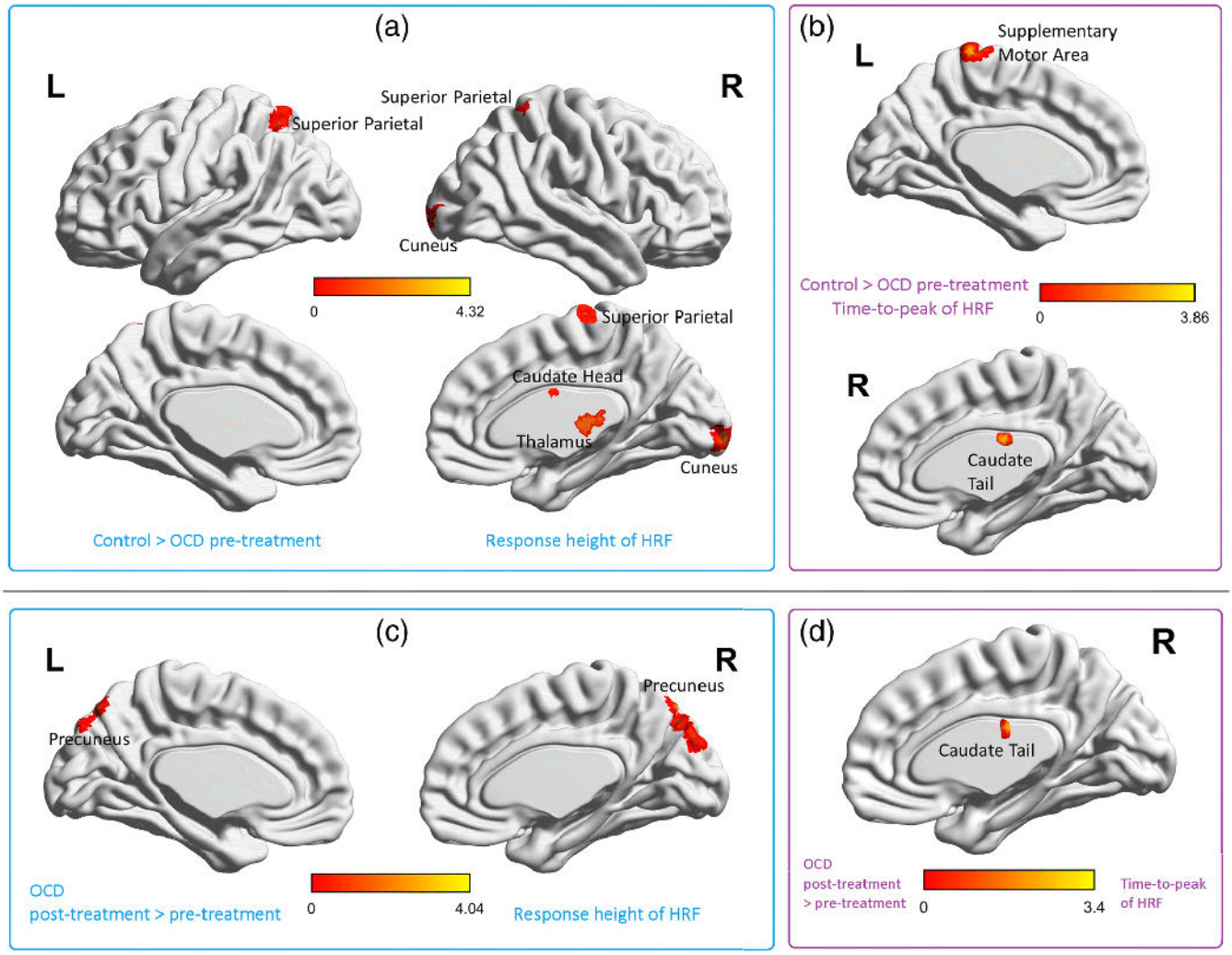

Fig.4.

Hemodynamic response function (HRF) findings for baseline healthy control > OCD pre-treatment comparison (a-b), and OCD post-treatment > pre-treatment comparison (c-d). **(a)** Brain regions with significant group differences in response height (RH) of the HRF. Thalamus (primarily pulvinar), caudate head, cuneus and superior parietal regions were abnormal in OCD before treatment, **(b)** Brain regions with significant group differences in time-to-peak (TTP) of the HRF. The caudate tail and supplementary motor area were abnormal in OCD pre-treatment. The color bars correspond to the T-values. Table 2 provides the coordinates, cluster volumes and statistics for these findings. **(c)** Brain regions with significant differences in HRF RH with treatment in OCD. Bilateral precuneus showed changes in the OCD group after treatment, **(d)** Brain regions with significant differences in TTP with treatment in OCD. The caudate tail showed changes in OCD post-treatment. The color bars correspond to the T-values. Table 2 provides the coordinates, cluster volumes and statistics for these findings. Pairwise T-tests with FWHM were not performed since it did not display significant group×time interaction (see Fig.S2 for FWHM ANOVA results).

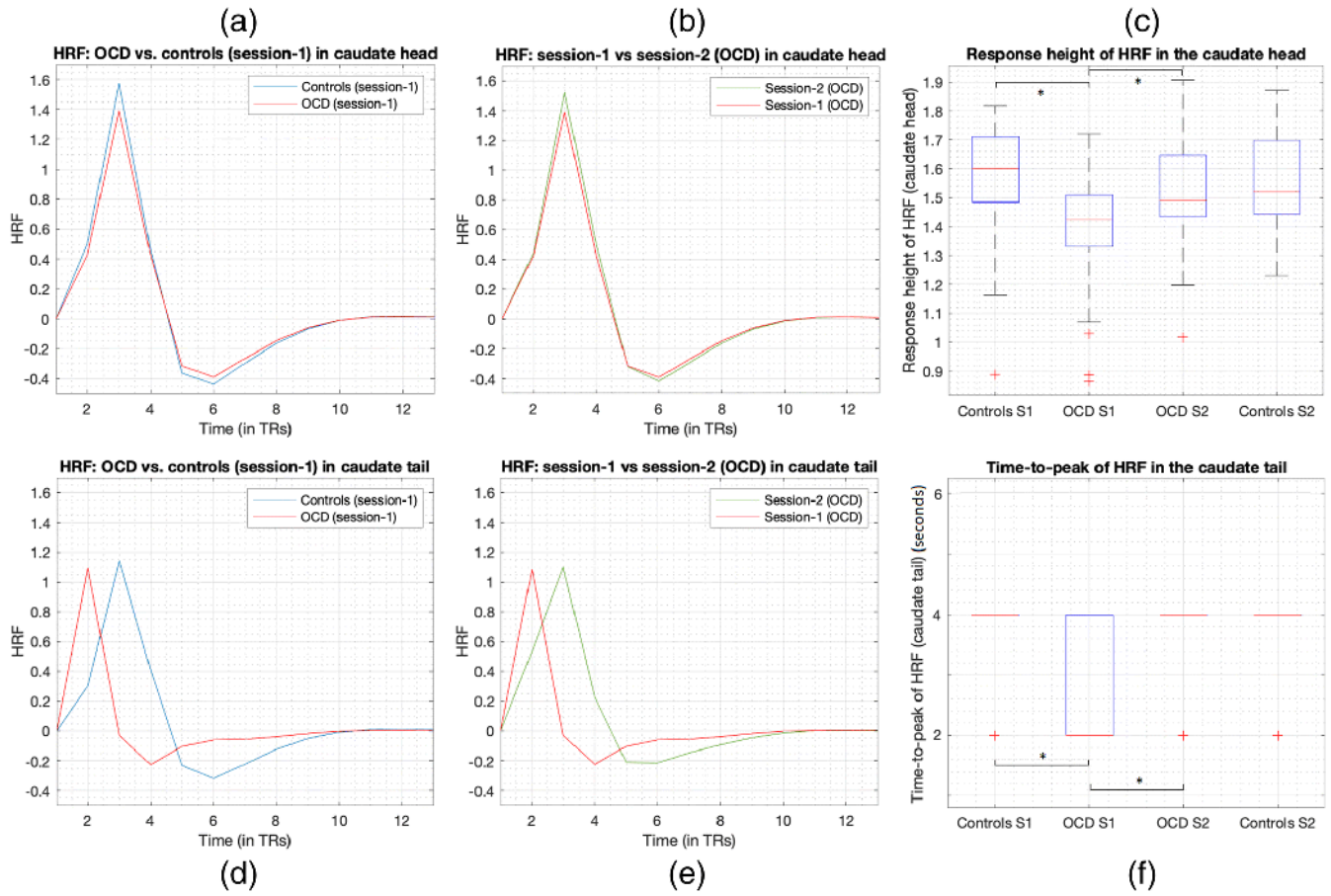

Fig.5.

HRF RH in the caudate head and TTP in the caudate tail were significantly lower in OCD at baseline and significantly increased with CBT treatment. Figures show the corresponding HRFs (averaged across subjects) and boxplots. Caudate head (top row, a-c): (**a**) HRFs at baseline in OCD and controls, (**b**) HRFs before (session-1 or S1) and after (S2) treatment in OCD, (**c**) boxplot showing lower RH in OCD at baseline and increased RH with treatment (OCD S2 and controls S2 were not significantly different). Caudate tail (bottom row, d-f): (**d**) HRFs at baseline in OCD and controls, (**e**) HRFs before and after treatment in OCD, (**f**) boxplot showing lower TTP in OCD (median=2s) at baseline and increased TTP with treatment (median=4s) (OCD S2 and controls S2 were not significantly different). In the boxplots, red line is the median, the box extends from 25th to 75th percentile, the dashed lines extend from minimum to maximum excluding outliers and the red '+' are the outliers. Note that since TR=2s, TTP could only assume values of multiples of 2s. For controls S1, controls S2, and OCD S2, TTP mostly assumed a value of 4s, because of which the interquartile range and median were 4s (blue lines and red line all coincide at 4s in the figure). In OCD S2, TTP predominantly assumed a value of 2s.

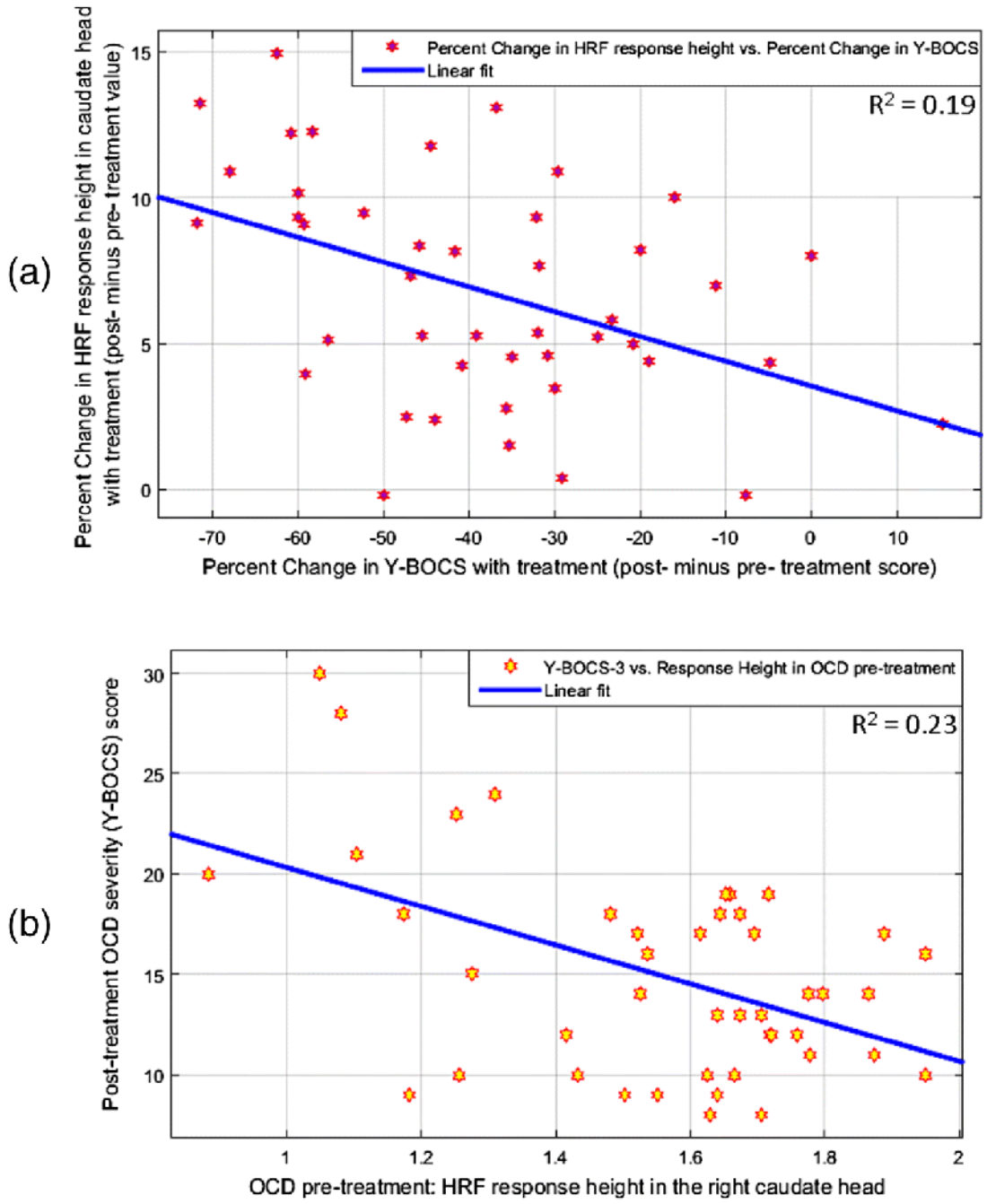

Fig.6.

Associations between the hemodynamic response function (HRF) parameters and OCD severity measured by the Yale-Brown Obsessive Compulsive Scale (YBOCS) in the caudate head. **(a)** Association between the percentage change in HRF response height (RH) with treatment (i.e. post-treatment minus pre-treatment RH) and the percentage change in YBOCS score with treatment. Larger increases in RH with treatment were associated with larger decreases in OCD severity. R=−0.4396, R^2=0.1932, P 0.0028. **(b)** Association

between RH pre-treatment and OCD severity post-treatment. Higher RH before treatment was associated with lower OCD severity after treatment. $R=-0.4790$, $R^2=0.2294$, $P= 0.0010$.

Table 1.

Demographics, clinical variables and comorbidities

	Healthy Controls (N=25)	OCD (N=44)	P-value
	Mean ± *SD*)		
Demographics			
Age (years)	30.76 ± 11.77	33.61 ± 11.20	0.32 [a]
Sex (male/female)	14/11	23/21	0.77 [b]
Education (years)	15.40 ± 2.24	15.68 ± 2.36	0.63 [a]
Clinical variables			
Handedness (percent right handed)	85 ± 19.83	86.6 ± 19.39	0.75 [a]
YBOCS (pre-treatment)	N/A	24.45 ±4.66	
YBOCS (post-treatment)	N/A	14.93 ±5.18	
HAMA (pre-treatment)	1.32 ± 1.22	12.23 ±5.44	< 0.001 [a]
HAMA (post-treatment)	1.08 ± 1.32	8.20 ± 5.13	< 0.001 [a]
MADRS (pre-treatment)	1.08 ± 1.22	15.09 ± 9.46	< 0.001 [a]
MADRS (post-treatment)	0.72 ± 1.14	10.61 ± 8.89	< 0.001 [a]

[a]The P-value was obtained by a two-sided t-test

[b]The P-value was obtained by a chi-squared test

OCD: obsessive-compulsive disorder; YBOCS: Yale-Brown obsessive-compulsive scale

MADRS: Montgomery-Ăsberg depression rating scale; HAMA: Hamilton anxiety rating scale

Table 2.

Names, coordinates and volume of the regions identified with HRF differences in this study using pairwise T-tests, along with the T-statistic. Tables are provided for both HRF parameters that showed a group×time interaction effect (response height and time-to-peak) for two comparisons: healthy controls at baseline > OCD pre-treatment, and OCD post-treatment > pre-treatment. Finally, the region which had time-to-peak differences for both the comparisons is shown. The coordinates and T-statistics correspond to the peak voxel within the region cluster.

Response Height: control>OCD (pre-treatment)						
	Vol. (mm^3)	**MNI Coordinates**			**AAL Region**	**T-stat**
1	576	18	−28	0	Thalamus_R	4.32
2	416	12	−98	4	Cuneus_R	4.07
3	320	18	4	22	Caudate_R	3.99
4	360	−26	−60	66	Parietal_Sup_L	3.53
5	336	28	−52	68	Parietal_Sup_R	3.52
Response Height: OCD post-treatment>pre-treatment						
	Vol. (mm^3)	**MNI Coordinates**			**AAL Region**	**T-stat**
1	624	−8	−78	44	Precuneus_L	4.04
2	496	8	−74	50	Precuneus_R	3.99
Time-to-peak: control>OCD (pre-treatment)						
	Vol. (mm^3)	**MNI Coordinates**			**AAL Region**	**T-stat**
1	**248**	**18**	**−18**	**24**	**Caudate_R**	**3.86**
2	520	−2	−28	74	Supp_Motor_L	3.83
Time-to-peak: OCD post-treatment>pre-treatment						
	Vol. (mm^3)	**MNI Coordinates**			**AAL Region**	**T-stat**
1	**96**	**20**	**−16**	**20**	**Caudate_R**	**3.39**